1

Common Compliant Platforms

Summary

This chapter presents details of the structural geometry of compliant offshore platforms while emphasizing the design and development of these platforms rather than of fixed platforms. Details of investigations carried out on the response control of a tension leg platform (TLP) and an articulated tower are presented. This chapter also presents various control strategies that are commonly deployed for response control of structures subjected to lateral loads while presenting detailed applications of tuned mass dampers (TMDs) in offshore structures. Experimental investigations and numerical analyses, reported by R. Ranjani (2015, "Response Control of Tension Leg Platform Using Tuned Mass Damper," PhD thesis, IIT Madras, India) and Prof. Deepak Kumar (Dept. of Ocean Engineering, IIT Madras, India) are sincerely acknowledged by the authors.

1.1 Introduction

While it is a common understanding that structural forms are conceived to counteract the applied loads acting on them, it may not be completely true in the context of offshore structures. This is due to the basic fact that offshore structures are designed to alleviate the encountered environmental loads based on their geometric form and not by the strength of the materials and structural properties based on the cross-section of the members. On the other hand, offshore structures are essentially form-dominant. Therefore, rigid-supported structural systems, which are conventionally good to transfer the applied loads to the foundations, are not attractive candidates for offshore structures. A few factors that influence

Offshore Compliant Platforms: Analysis, Design, and Experimental Studies,
First Edition. Srinivasan Chandrasekaran and R. Nagavinothini.

This Work is a co-publication between John Wiley & Sons Ltd and ASME Press.

the choice of the geometric form of offshore structures are a structural form with a stable configuration, and a geometric form with low installation, fabrication, and decommissioning costs; that leads to lower capital expenditures (CAPEX) and a higher return on investment (ROI). The result is an earlier start for production and greater mobility, and a platform that requires the least intervention so that uninterrupted production can take place.

Offshore structures are grouped as fixed, compliant, and floating types, based on the boundary conditions of their station-keeping characteristics. Fixed platforms are further categorized as jacket platforms, gravity platforms, and jack-up rigs. Compliant platforms are further categorized as guyed towers, articulated towers, and tension leg platform (TLPs). Floating platforms are further categorized as semi-submersibles, floating production units (FPUs), floating storage and offloading (FSO), floating production storage and offloading (FPSO), and spar. While fixed platforms are designed to remain insensitive to lateral loads that arise from waves, wind, currents, and earthquakes, these platforms are expected to resist the encountered loads using both their material strength and structural redundancy. A strength-based design approach is more popular for use when designing such platforms, as they exhibit very low displacement under lateral loads. These structural forms are also stable due to their massive weight, which is an advantageous design factor. However, with regard to the other factors that influence the choice of the structural forms of offshore structures, as explained earlier, fixed platforms are least preferred for deepwater construction. Table 1.1 shows a list of fixed platforms constructed worldwide (Srinivasan Chandrasekaran 2017).

It is interesting to note that offshore engineers gradually realized that restricting the motion of the platform by making it fixed to the seabed was not necessary. Instead, conceptual developments were focused on flexible structural forms and gave birth to compliant structures. Further, fixed platforms became increasingly expensive and difficult to commission in greater water depths. Hence, a modified design concept was evolved in offshore structural forms, which focused on flexible systems; it gave rise to compliant offshore structures. The word *compliance* refers to flexible systems. Fixed platforms were designed to encounter the environmental loads with their strength and fixity (rigidness, obtained from both large member dimensions and fixity to the seabed).

On the other hand, compliant-type offshore platforms are allowed to undergo large displacements but are position-restrained using cables or tethers. In addition to the material strength that helps to counter environmental loads, a major contribution came from the relative displacement concept of the design: compliant offshore platforms do not resist loads based on their fixity to the seabed but rather receive lesser loads due to their motion characteristics.

Table 1.1 Major fixed platforms constructed worldwide (as of 2017).

S. no	Platform name	Water depth (m)	Location
	North America		
1	East Breaks 110	213	USA
2	GB 236	209	USA
3	Corral	190	USA
4	EW910-Platform A	168	USA
5	Virgo	345	USA
6	Bud Lite	84	USA
7	Falcon Nest	119	USA
8	South Timbalier 301	101	USA
9	Ellen	81	USA
10	Elly	81	USA
11	Eureka	213	USA
12	Harmony	365	USA
13	Heritage	328	USA
14	Hondo	259	USA
15	Enchilada	215	USA
16	Salsa	211	USA
17	Cognac	312	USA
18	Pompano	393	USA
19	Bullwinkle	412	USA
20	Canyon Station	91	USA
21	Amberjack	314	USA
22	Bushwood	***	USA
23	Hebron	92	Canada
24	Hibernia	80	Canada
25	Alma	67	Canada
26	North Triumph	76	Canada
27	South Venture	23	Canada
28	Thebaud	30	Canada
29	Venture	23	Canada
30	Ku-Maloob-Zaap (KMZ)	100	Mexico

(*Continued*)

Table 1.1 (Continued)

S. no	Platform name	Water depth (m)	Location
		South America	
1	Peregrino Wellhead A	120	Brazil
2	Hibiscus	158	Trinidad and Tobago
3	Poinsettia	158	Trinidad and Tobago
4	Dolphin	198	Trinidad and Tobago
5	Mahogany	87	Trinidad and Tobago
6	Savonette	88	Trinidad and Tobago
7	Albacora-Leste	***	Peru
		Australia	
1	Reindeer	56	Australia
2	Yolla	80	Australia
3	West Tuna	***	Australia
4	Stag	49	Australia
5	Cliff Head	**	Australia
6	Harriet Bravo	24	Australia
7	Blacktip	50	Australia
8	Bayu-Undan	80	Australia
9	Tiro Tiro Moana	102	New Zealand
10	Lago	200	Australia
11	Pluto	85	Australia
12	Wheatstone	200	Australia
13	Kupe	35	New Zealand
		Asia	
1	QHD 32-6	20	China
2	Penglai	23	China
3	Mumbai High	61	India
4	KG-8	109	India
5	Bua Ban	***	Thailand
6	Bualuang	60	Thailand
7	Arthit	80	Thailand
8	Dai Hung Fixed Well head	110	Vietnam
9	Ca Ngu Vang	56	Vietnam

Table 1.1 (Continued)

S. no	Platform name	Water depth (m)	Location
10	Chim Sao	115	Vietnam
11	Oyong	45	Indonesia
12	Kambuna	40	Indonesia
13	Gajah Baru	***	Indonesia
14	West Belumut	61	Malaysia
15	Bukha	90	Oman
16	West Bukha	90	Oman
17	Al Shaheen	70	Qatar
18	Dolphin	***	Qatar
19	Zakum Central	24	UAE
20	Mubarek	61	UAE
21	Sakhalin-I	***	Russia
22	Lunskoye-A	48	Russia
23	Molikpaq	30	Russia
24	Piltun-Astokhskoye-B	30	Russia
25	LSP-1	13	Russia
26	LSP-2	13	Russia
27	Gunashli Drilling and Production	175	Azerbaijan
28	Central Azeri	120	Azerbaijan
29	Chirag PDQ	170	Azerbaijan
30	Chirag-1	120	Azerbaijan
31	East Azeri	150	Azerbaijan
32	West Azeri	118	Azerbaijan
33	Shah Deniz Production	105	Azerbaijan
	Europe		
1	Brage	140	Norway
2	Oseberg A	100	Norway
3	Oseberg B	***	Norway
4	Oseberg C	***	Norway
5	Oseberg D	100	Norway
6	Oseberg South	100	Norway
7	Gullfaks A	138	Norway

(*Continued*)

Table 1.1 (Continued)

S. no	Platform name	Water depth (m)	Location
8	Gullfacks B	143	Norway
9	Gullfacks C	143	Norway
10	Sleipner A	80	Norway
11	Sleipner B	**	Norway
12	Sleipner C	***	Norway
13	Valhall	70	Norway
14	Ekofisk Center	75	Norway
15	Varg Wellhead	84	Norway
16	Hyperlink	303	Norway
17	Draugen	250	Norway
18	Statfjord A	150	Norway
19	Statfjord B	***	Norway
20	Statfjord C	290	Norway
21	Beatrice Bravo	290	UK
22	Jacky	40	UK
23	Ula	40	UK
24	Inde AC	70	UK
25	Armada	23	UK
26	Auk A	88	UK
27	Fulmar A	84	UK
28	Clipper South	81	UK
29	Clair	24	UK
30	Brae East-I	140	UK
31	Lomond	113	UK
32	Brae East-II	86	UK
33	Alwyn North A	126	UK
34	Alwyn North B	126	UK
35	Cormorant Alpha	126	UK
36	Dunbar	145	UK
37	Nelson	***	UK
38	Schooner	100	UK
39	Andrew	117	UK

Table 1.1 (Continued)

S. no	Platform name	Water depth (m)	Location
40	Forties Alpha	107	UK
41	Forties Bravo	107	UK
42	Forties Charlie	107	UK
43	Forties Delta	107	UK
44	Forties Echo	107	UK
45	Eider	159	UK
46	Elgin	93	UK
47	Elgin PUQ	93	UK
48	Franklin	93	UK
49	Babbage	42	UK
50	Alba North	158	UK
51	Alba South	138	UK
52	Judy	80	UK
53	Amethyst	30	UK
54	Buzzard	100	UK
55	Brigantine BG	29	UK
56	Brigantine BR	***	UK
57	Cecilie	60	Denmark
58	Nini East	***	Denmark
59	Nini	58	Denmark
60	South Arne	60	Denmark
61	Galata	34	Bulgaria

Compliant offshore platforms are position-restrained by cables or tethers. A high pre-axial loaded tether offers resistance to lateral loads while counteracting the large buoyancy force. Therefore, in the strength-based design, the concept is shifted toward a displacement-controlled design. Large displacements allowed in the design demand a recentering ability for the platform. *Elasticity* refers to material characteristics and ensures that a member regains its form, shape, and size when the applied load is within the elastic limit and is removed, and *recentering* is an extension of this property. Recentering refers to the capability of the structural form (not a material characteristic) to regain its initial position (which may not be an equilibrium position) in the presence of external forces (not when they are removed, unlike elasticity). This is very important in the context of compliant platform design, because large displacements are permitted as a part of the design. Apart from ensuring the attainment of the original position, recentering ensures the safety of other existing appurtenances and auxiliary fixtures like risers, pipelines, electric cables, and umbilicals that are connected to the compliant platform.

One of the fundamental differences between elasticity and recentering is that the former is a material characteristic, while the latter is a geometric characteristic. Design of the geometric form of compliant structures is principally dominated by balancing the buoyancy force and weight of the platform. While a preferred design is to make the buoyancy force exceed the weight, because this can enable easy installation, the difference between the two forces is balanced by an external axial force on the tethers (or cables) as pre-tension. Large displacements of compliant platforms invoke the participation of the added mass of the body through a variable submergence effect. It helps restore the dynamic equilibrium in the system in the presence of various environmental loads. One of the most successful structural forms of compliant offshore platforms is the TLP.

1.2 Tension Leg Platforms

Several TLP design concepts have been developed as the result of research and studies done on various elements of TLPs, which makes them suitable for different environments. TLPs operate successfully in deep waters and are installed at depths of a few thousand meters; they are classified as hybrid compliant structures that are suitable for both drilling and production operations.

A conventional TLP has four legs, called *columns*. The four columns are connected with a pontoon ring at the base of the column, as shown in Figure 1.1. A square or rectangular deck is placed at the top of the columns. The TLP is held in position with the help of taut, moored, pre-tensioned tethers that connect the platform columns to the seabed through the pile templates. Due to the excess buoyancy of the TLP, the tethers are always in pre-tension. A structure can have six degrees of freedom (DOF): three translation motions and three rotational motions. TLPs are designed in a way that tension in the tethers allows horizontal motion but restricts vertical motion. Hence TLPs are flexible in the surge, sway, and yaw DOF, while the heave, pitch, and roll DOF are restrained. Thus TLPs have high natural periods in the surge, sway, and yaw DOF, and low natural periods in the heave, pitch, and roll DOF. TLPs are designed such that the natural periods are far separated from the wave frequency band. The heave natural period is reduced by increasing the pipe wall thickness of the tethers, and the natural pitch period is decreased by the spacing of the tethers.

Figure 1.1 A typical tension leg platform.

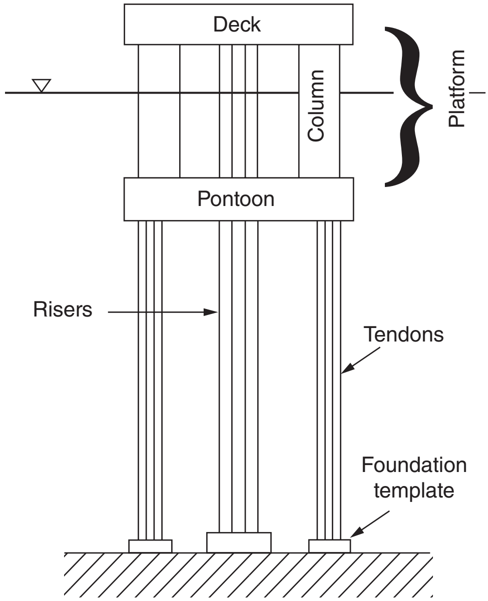

When no load is applied to the structure, the structure is in a stationary, stable condition. Due to excess buoyancy, the tethers are in high tension, so the platform is held down to the seabed. Given lateral loading from wind, waves, or currents, the structure experiences a lateral displacement. This lateral displacement of the TLP is called *offset*. The offset condition of the TLP pulls down the structure. The vertical displacement is called *setdown*. Since the tethers are in high tension, the setdown effect is minimal. The horizontal component of the pre-tension in the tethers produces a restoring force to the structure, bringing the hull back to its original position. There is a tension variation, which is due to the variable submergence effect. This flexibility of the TLP in horizontal DOF creates nonlinearity in the stiffness of the structure due to large displacements. This phenomenon affects the dynamics of the entire structural system. A schematic diagram of TLP setdown is shown in Figure 1.2. During this phenomenon, there are changes in the tension of the tethers. Arbitrary displacement of the TLP produces dynamic tether-tension variation.

Compliancy of TLPs, introduced in the design of the structural form, enables the effective negotiation of encountered environmental loads (Adrezin et al. 1996; El-gamal et al. 2013). Analytical studies carried out on TLPs showed that high elasticity of tethers controls the motion response of TLPs through a lesser variation in tether tension (Bar-Avi 1999; Booton et al. 1987; Mekha et al. 1996). Methods for motion response analyses were addressed, and the method for the

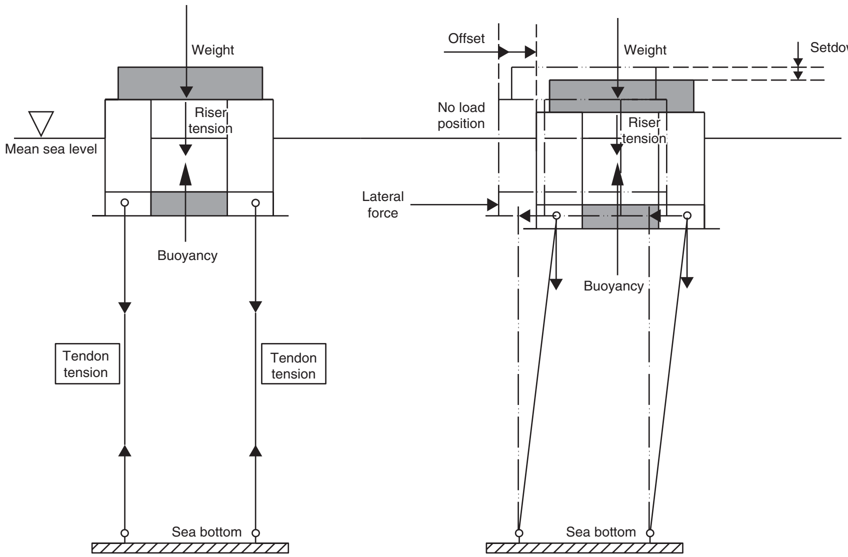

Figure 1.2 TLP mechanics.

structural design was also discussed based on fatigue analysis and other design procedures (Chandrasekaran and Jain 2002a, b, 2004; Chandrasekaran et al. 2004, 2007a, b, 2011). The influence of variable submergence on added mass terms and the coefficients of the stiffness matrix were addressed in addition to the stability analysis (Chandrasekaran et al. 2006b, 2007c; Kim et al. 2007). The results were compared with those of an eight-legged jacket structure and guyed tower by highlighting the advantages of TLP.

Jefferys and Patel (1982) studied the Mathieu instability of a TLP in sway motion using an energy-balance technique. Predicted sway motions were within the acceptable limits even in the presence of large waves, which were caused by Mathieu excitation (Donely and Spanos 1991; Ertas and Lee 1989; Ertas and Eskwaro-Osire 1991). The results showed that square law variation of fluid damping influenced the upper bound of the amplitude of oscillation. Yoneya and Yoshida (1982) carried out experimental investigations on the dynamic response of a TLP to regular waves in a wave tank. Numerical analysis was carried out on a full-scale model in real sea conditions to extrapolate the response behavior of the prototype under operational sea conditions. The analytical methods were validated and compared with the experimental results. Patel and Lynch (1983) developed a mathematical model to study the coupled dynamics of a tensioned buoyant surface platform with taut tethers. The results show that the platform response is influenced by tether dynamics with long tethers in comparison to the water depth and payload, respectively (Chandrasekaran and Gaurav 2008). de Boom et al. (1984) carried out experiments on scale models with both regular and irregular waves. Time-domain based potential theory was used to predict motion and tether forces on a TLP. The results of the analytical and experimental studies were in good agreement except for a few discrepancies at low frequencies. The reasons were attributed to the estimation of the wave in the presence of drift forces, and improper modeling of the second harmonics of tether tension given regular waves at low frequencies (Chou 1980; Gasim et al. 2008; Ramachandran et al. 2014). Smiu and Leigh (1984) discussed the analysis methodology to estimate the surge response to turbulent wind in the presence of current and waves; nonlinearities arising from hydrodynamic forces were included in the analysis. An alternate wind spectrum with ordinate at the origin is used by several researchers to account for the fluctuations in wind speed at very low frequencies (Jain and Srinivasan Chandrasekaran 2004; Kurian et al. 2008; 1993; Leonard and Young 1985; Logan et al. 1996). The results show that given extreme wave conditions, significant wind-induced resonant amplification effects occurred even for small drag coefficient in the Morison equation (Jain 1997; Kobayashi et al. 1987; O'Kane et al. 2002).

Spanos and Agarwal (1984) studied the response of a TLP model given wave forces at the displaced position of the platform by modeling a TLP as a single degree of freedom (SDOF) system. The Morison equation was used to predict wave forces on the structure, and the equation of motion was solved by the numerical integration method. It was shown that the proposed simplified method remains valid for both deterministic and stochastic wave loads. Yoshida et al. (1984) presented the equations for the linear response analysis method with regular waves to find the response motion. Tension variations of tendons and structural member forces were solved for the structural response of a TLP, and this method was confirmed by comparison with the test results on two small-scale TLP models simultaneously. Leonard and Young (1985) presented the coupled response of compliant offshore structures with examples of articulated towers, guyed towers, and TLPs. Three-dimensional finite element analysis (3D FEA) was used to simulate the static and dynamic coupled responses. It was concluded that the procedure used in the study requires a longer time for simulation in the case of a TLP using the Morison equation to predict the wave forces for all of the considered compliant structures (Jefferys and Patel 1982; Mercier et al. 1997; Muren et al. 1996).

Booton et al. (1987) and Yashima (1976) conducted a parametric study to estimate the effect of tether damage on a TLP by reducing tether in the presence of regular waves at a water depth of 160 m without changing the pre-tension. Nonlinear analytical results also showed that the amplitudes of the motion were more than the linear analyses results the lateral motion of the platform was not influenced by the loss of tether stiffness but increased heave response was observed (Perryman et al. 1995; Vickery 1990). Kobayashi et al. (1987) performed a study on the dynamic response of a TLP to random waves; experiments and analytical studies were performed with time and frequency domains using three-dimensional singularity distribution methods to determine the wave forces and concluded that the time domain analytical results compared well with the experimental results. Nordgren (1987) studied the dynamic response of a TLP using spectral analysis closer to natural heave, pitch, and roll periods of vertical DOF of the exciting waves; resonant response and the fatigue life of tethers were examined. They concluded that the resonant response is reduced by the combined effect of radiation damping and material damping of tethers.

Ertas and Lee (1989) carried out a stochastic analysis of a TLP given random waves in the presence of constant current velocity. A modified Morison equation was used to estimate wave forces considering the relative motion in both the drag and inertia terms, while the superposition method was used for random waves in the time domain. The responses of a TLP in surge DOF with and without current were compared, and the conclusion was that the frequency domain analysis technique was quite efficient. Vickery (1990) studied the response of a TLP in the presence of the combined wind and wave loads; experimental studies were conducted on 1 : 200 scale model in a wind-wave flume with scaled wind and wave loads. First- and second-order wave loads were estimated using the Morison equation and diffraction theory in the numerical model, respectively. Wind loads were estimated using quasi-static theory (Davenport 1961). The equation of motion was solved using the fourth-order Runge–Kutta differential equation solver in the time domain. Based on the studies, it was concluded that the surge response due to wind loads dominates the overall response of a TLP.

Roitman et al. (1992) reported the experimental responses of a small-scale model of a TLP in deep water and compared the results with the numerical model. The results confirmed that the study of numerical simulations for the effects of impact loads and wave loads are performed well. Kurian et al. (1993) conducted experimental studies on a scaled TLP in the presence of regular and random waves with different wave directions. They showed that TLPs exhibited a satisfactory response control and were suitable for deepwater applications (Low 2009; Yan et al. 2009; Younis et al. 2001). Adrezin et al. (1996) reviewed the dynamic response of different compliant offshore structures with the highlights of various modeling approaches of TLPs in the presence of wind, wave, and current forces.

Mekha et al. (1996) performed a nonlinear coupled analysis to study the implication of tendon modeling on the response of a TLP. The tendons were modeled as mass-less elastic springs that were connected to the hull. The responses of TLPs in different water depths were studied, and the results also showed that tether tension variation was on the order of 10% of the initial pre-tension value (Tabeshpour et al. 2006; Thiagarajan and Troesch 1998; Vannucci 1996). It was concluded that the lateral stiffness of the TLP should be modeled carefully to predict the lateral response. Logan et al. (1996) conducted a feasibility study on a three-column concrete mini TLP for marginal deepwater fields and showed that it is technically and economically superior as compared to other floating platforms. Alternative concepts such as one-column TLPs, two-column TLPs, and three-column TLPs with steel truss pontoons were considered for the study; they reported that a three-column TLP is the optimum solution for marginal fields (Zeng et al. 2007). Murray and Mercier (1996) performed hydrodynamic tests on 1 : 25 scale model of an Ursa TLP with truncated tendons. The study highlighted the importance of model tests for predicting the responses of deepwater TLPs.

Muren et al. (1996) presented a three-column TLP design for 800 m water depth, which is easily extended to 1500 m with minimal time and cost. The dynamic response was computed using a radiation-diffraction code augmented with linearized Morison elements; model tests at 1 : 100 scale were carried out to verify the numerical prediction. Vannucci (1996) proposed a simplified method to design an optimal TLP depending on two variables, such as effective structure and dimensions of the hull, to obtain required buoyancy. The results agreed well with the available data. Jain (1997) performed a nonlinear time-history analysis using Newmark's method to study the coupled response of offshore TLPs in the presence of regular waves. Airy wave theory was used to estimate water particle kinematics, and the Morison equation was used to estimate the wave forces by neglecting diffraction effects. Mercier et al. (1997) conducted tests on a scale model of a Mars TLP in the presence of waves, wind, and current loads. A 1 : 55 scale ratio was chosen for towing tests that were carried out at three different drafts to ensure floatation stability, while hydrodynamic tests were carried out on a 1 : 200 scale model. Numerical analysis was performed to validate the experimental results, which were subsequently considered in the global design of the Mars TLP. Chakrabarti (1998) addressed different models' similitude, techniques, deepwater testing requirements, environments, and areas of testing. Thiagarajan and Troesch (1998) conducted model tests to examine the effects on TLP columns in the presence of waves with uniform current. The results showed that the heave damping induced due to the disk was linear for the amplitude of oscillation. Bar-Avi (1999) studied the response of a TLP given various environmental loads such as wind, wave, seismic force, and current by considering geometric and external force nonlinearities. Based on the studies, the importance of such analyses was highlighted for the commissioning of the structure. Buchner et al. (1999) combined the requirements of water depth, wave, wind and current generation, hydraulic design, and wave absorption in a deepwater offshore basin to conduct experiments on deepwater and ultra-deepwater structures. Niedzweki et al. (2000) estimated surface wave interactions with a compliant deepwater mini-TLP and two spar platforms by using analytical expressions and a series of model tests. The Weibull distribution was employed on the prediction of the response histogram, and the analytical results compared well with the experimental results. Younis et al. (2001) proposed fundamental equations that govern the turbulent flow based on computational fluid dynamics and an alternate method to estimate hydrodynamic forces on a full-scale mini TLP. The results obtained from both methods were compared with the experimental data observed on 1 : 70 scale models, and they showed good agreement for the front column members of a TLP. Stansberg et al. (2002) reviewed the challenges in verifying hydrodynamic forces computed on deepwater structures. Model tests with truncated moorings were carried out, and the results were compared with those obtained using computer simulations and other hybrid approaches. The results highlighted the complexities and limitations of each of the investigation methods in addition to the future challenges associated with them.

Chandrasekaran and Jain (2002a) compared the dynamic behavior of square and triangular TLPs given regular wave loading. The results show that a triangular TLP exhibits a lower response in the surge and heave DOF than that of a four-legged (square) TLP. It was also reported that the pitch response of a triangular TLP was more than that of a four-legged (square) TLP. Chandrasekaran and Jain (2002b) investigated the dynamic response of a triangular TLP in the presence of random sea waves. The random sea waves were generated using the Pierson-Moskowitz (PM) spectrum with different significant wave heights and peak periods. Airy theory was used for water particle kinematics. Morison theory was used for wave force estimation, and the equation of motion was solved using the Newmark-beta method. The effect of current was also investigated, with the conclusion that the coupling responses of the structure were greater given the combined effect of wave and current. O'Kane et al. (2002) proposed a new method for estimating the added mass and hydrodynamic damping coefficients of a TLP. Model tests were conducted on one, two, and four columns of a TLP, with the conclusion that based on the Keulegan–Carpenter number, a TLP with multiple columns behaves identically to a single-column TLP with respect to the damping ratio estimates.

Bhattacharyya et al. (2003) reported on the coupled dynamics of a SeaStar mini TLP using Morison type wave loading at two water depths: 215 and 1000 m. Experimental investigations were performed for a scale model corresponding to 215 m water depth for validation of the numerical model. The response amplitude operators (RAOs) of the SeaStar at two water depths were compared to highlight limitations related to the experimental investigations by indicating the influence of water depth on the response of a TLP. Liagre and Niedzwecki (2003) estimated the coupled responses of a TLP in the time and frequency domains by considering nonlinear effects such as nonlinear stiffness, inertia, and damping forces. They verified the numerical results obtained from WAMIT with those of the experimental measurements. Chandrasekaran et al. (2004) studied the influence of hydrodynamic drag and inertia coefficients on the response behavior of triangular

TLPs in the presence of regular waves. The response of two triangular TLPs at 600 and 1200 m water depths were compared; drag and inertia coefficients were assumed based on the Reynolds and Keulegan–Carpenter numbers. Wave forces were estimated using the modified Morison equation while neglecting diffraction effects. Based on the studies, it was concluded that the influence of hydrodynamic coefficients was greater in the case of a 15 second wave period than a 10 second wave period.

Jain and Chandrasekaran (2004) performed numerical analyses to study the aerodynamic behavior of a triangular TLP due to low-frequency wind force and random waves. They included various nonlinear effects such as variable submergence, hydrodynamic force, tether tension, etc. in the study. Wave forces were estimated using the Morison equation and Airy wave theory, while wind force was estimated using Emil Simiu's wind velocity spectrum. Based on the study, it was concluded that low-frequency wind force alters the response of a triangular TLP significantly. Stansberg et al. (2004) suggested advanced numerical tools for model studies associated with ultra-deepwater structures that arise from the limitations caused by water depth in existing wave tanks. A model-the-model procedure and the final prototype simulations were presented. Chandrasekaran et al. (2006a) investigated the seismic analysis of a triangular TLP in the presence of moderate regular waves by considering nonlinearities due to the change in tether tension and nonlinear hydrodynamic drag forces. El Centro and Kanai-Tajimi's earthquake data were considered for the analysis, and the vertical ground displacement was imposed as the tether tension variation. Based on the studies, it was concluded that the TLP heave response was affected and found to vary nonlinearly. Chandrasekaran et al. (2006b) conducted the numerical studies on TLPs; the water depth increases with deepwater-compliant structures, and tether tension variation plays an important role in the stability analysis of TLPs. Lower pre-tension values, as shown in the Auger TLP, lead to instability. Triangular TLPs with three groups of tethers are more stable than four-legged TLPs in the first fundamental mode of vibration.

Tabeshpour et al. (2006) developed a computer program called STATELP using MATLAB to perform a nonlinear dynamic response analysis of a TLP in both the time and frequency domains given random sea wave loading. The PM spectrum was used to generate the random waves; the modified Morison equation and Airy theory were used to predict the wave loads. The power spectral density (PSD) functions of displacement, velocity, and acceleration were calculated from the nonlinear responses in different DOF, and the safety of personnel and facilities on board were examined. Xiaohong et al. (2006) developed a numerical code called COUPLE to study the dynamic response of TLPs, including the tendons and risers. The comparisons of experimental and numerical results showed that wave loads on a mini TLP were accurately predicted using the Morison equation and also concluded that COUPLE was able to predict the dynamic interaction between the hull and its tendon and riser systems while the related quasi-static analysis fails. Bas Buchner and Tim Bunnik (2007) investigated the effect of extreme wave loads on the response of floating structures resulting from the air gap, green water on the deck, and slamming to the hull. Green-water effects were studied on floating FPSOs, and dynamic response studies were studied on a TLP using experimental and time integration analytical investigations. The improved volume of fluid method was adopted in the time domain analysis to predict the green-water effect. Based on the studies, it was concluded that extreme waves could damage the floating structure due to the air gap, green water on the deck, or slamming to the hull. The experimental and analytical predictions compared well. Chandrasekaran et al. (2007a) presented the response behavior of triangular TLPs in the presence of regular waves using Stokes fifth-order nonlinear and Airy wave theories. The wave forces were estimated using the modified Morison equation. The drag and inertia coefficients were varied along with the depth of the TLPs. The results showed that the responses were higher when Airy wave theory was considered than with Stokes wave theory. Chandrasekaran et al. (2007b) performed a dynamic analysis of two different triangular TLPs at 527.8 and 1200 m water depths with 45° inclined impact load and wave loads. The impact load was considered as triangular and half-triangular loads. The wave force was estimated using the modified Morison equation and Stokes fifth-order wave theory. The results indicated that the impact load significantly affected the response when it acted on the columns rather than the pontoons.

Chandrasekaran et al. (2007c) studied the response behavior of triangular TLPs using the dynamic Morison equation considering nonlinearities associated with vortex shedding effects, variable submergence, variable added mass, stiffness, damping, and variable hydrodynamic coefficients along with the depth of the columns. The wave force was estimated using Stokes fifth-order nonlinear wave theory. Based on the studies, it was concluded that the triangular TLP responses were higher in deeper water, and the dynamic Morison equation was capable of estimating vortex shedding effects on the columns. Cheul-Hyun Kim et al. (2007) developed a numerical code to study the response of a TLP in the presence of regular waves by assuming the TLP as a flexible model. Source distribution and radiation effects were considered in the analysis. The numerical results compared well with the established experimental and analytical results. Zeng et al. (2007) modeled an International Ship Structures Congress (ISSC) TLP for its displacement, mass, and tether tension. The equation of motion was solved in the time domain by considering nonlinearities such as instantaneous wet surface, submerged volume, displacement, velocity, and acceleration of the structure. The responses were compared with the published results and verified well. Chandrasekaran and Gaurav (2008) performed an earthquake motion analysis on three different triangular TLPs in the presence of high sea waves. Seismic excitation was generated using the Kanai-Tajimi earthquake spectrum. The results showed that the tension variation of the tethers given the combined loads was higher than the regulation values, and TLPs in deeper water showed lesser responses. Gasim et al. (2008) developed MATLAB coding to study the dynamic response of square and triangular TLPs in the presence of random waves. Airy wave theory and the Morison equation were used to estimate wave force. A time history analysis was performed using the Newmark-beta method, and RAOs of a square TLP were compared with the established results to validate the MATLAB code. The study was extended to triangular TLPs, and the RAOs of the square and triangular TLPs were compared. The results showed that except for surge RAO, all the responses of triangular TLPs were higher than those of square TLPs.

Kurian et al. (2008) developed a MATLAB program to study the nonlinear response of a square TLP at 300 m water depth in the presence of regular and random waves. Airy wave theory and the Morison equation were used to determining the wave loading. The Newmark-beta method was used to solve the equation of motion. The numerical results were extended to 600 m water depth and predicted higher responses at 600 m water depth. The RAOs compared well with the available experimental and theoretical results. Low (2009) performed a frequency domain analysis of a TLP by linearizing the system. Wave forces were computed using WAMIT. Four separate cases with different static offsets were studied. The linearization technique agreed well with the time domain results with a few limitations. Yan et al. (2009) compared the experimental and analytical stress response amplitudes of a TLP under extreme environmental loads. The analytical predictions were done in WAMIT. Strain gauges were placed on the model to measure the strain record of the platform. Stress RAOs were plotted using a fast Fourier transform technique, and the experimental and analytical results were compared. Jayalekshmi et al. (2010) presented a nonlinear program using Lagrangian coordinates and Newmark integration methods to investigate the effect of tether-riser dynamics on the response of deepwater TLPs at 900 and 1800 m water depths in the presence of random waves. Linear wave theory and the Morison equation were used to estimate the wave forces; current forces were also considered in the analysis. Based on the results, it was concluded that the response of the TLP was high at 1800 m water depth. Chandrasekaran et al. (2010) stated that ringing waves are highly nonlinear and contain strongly asymmetric transient waves; hence the shape of such waves becomes critical in offshore compliant structures and is presented along with the method of analysis. Frequency responses were observed to be almost the same for all cases, indicating that all platforms showed ringing as the peaks are not observed near the corresponding natural frequencies. This study develops a mathematical formulation of the impact waves responsible for ringing and examines their influence on offshore TLPs with different geometric configurations located at different water depths.

Chandrasekaran et al. (2011) developed a mathematical formulation of impact and non-impact waves and discussed the method of analysis for triangular TLPs. Their effects are more comparable to square TLPs. Impact and non-impact waves are responsible for ringing and springing phenomena, respectively. Ringing (caused by impact waves in the pitch DOF) and springing (caused by non-impact waves in the heave DOF) in both platform geometries are undesirable because they present a serious threat to platform stability. Analytical studies show that equivalent triangular TLPs positioned at different water depths are less sensitive to these undesirable responses, thus making them a safe alternative for deepwater oil explorations.

El-Gamal et al. (2013) presented numerical studies for square TLPs using the modified Morison equation; they were carried out in the time domain with water particle kinematics using Airy linear wave theory to investigate the effect of changing the tether tension force on the TLP. The Newmark-beta integration method was used to solve the nonlinear equation. The surge response showed high-amplitude oscillations that were significantly dependent on wave height, and indicated that special attention should be given to tether fatigue because of the tethers' high tensile static and dynamic stress. Chandrasekaran et al. (2013) quantified the response variations of a triceratops – a new-generation offshore platform that alleviates wave loads with its innovative structural form and design. In the presence of seismic activities, the proposed new-generation offshore platforms are very useful. While they are positively buoyant, the platform is position-restrained by tethers and ball joints. Ball joints connect the deck and the buoyant leg structure (BLS) units and also restrain the transfer of rotations between them. These platforms experience significant tether-tension variation given vertical seismic excitations caused at the seabed (Ney Roitman et al. 1992; Chandrasekaran et al. 2006a). Records of the El Centro earthquake and the artificially generated earthquake using the Kanai-Tajimi (K-T) power spectrum are considered for the study. Chandrasekaran et al. (2013) develop a mathematical formulation for the aerodynamic analysis of an offshore triceratops and examines its response in the presence of regular waves and wind. Based on the numerical studies conducted here, it is observed that the triceratops shows a significant reduction in deck response, with no transfer of rotation from the BLS; the deck remains horizontal given the encountered wave loads. The response of the deck is relatively lower than in the BLS units in the pitch and yaw DOF even at higher significant wave heights. The geometric form is advantageous for keeping more facilities on the deck system and operating even given moderate weather conditions. Chandrasekaran et al. (2015) develop an offshore triceratops. Experimental studies are performed to study the dynamic response of the triceratops in coupled DOFs given regular waves with a unidirectional wave on the scale model. Higher natural periods in the surge, sway, and heave DOF of the triceratops indicate a higher degree of compliance in comparison to other compliant type offshore platforms like TLPs. Numerical studies are also carried to verify the experimental results and dynamic responses of the triceratops in the presence of different wave headings for regular and random waves. Based on the detailed investigations carried out, it is seen that the coupled responses of the deck in the rotational DOF are less than those of the buoyant legs.

Ramachandran et al. (2014) implemented a three-dimensional fully coupled hydro-aero-elastic model for a floating TLP wind turbine with 17 DOF. The aerodynamic loads were implemented using unsteady blade element momentum theory, which includes the effect of a moving tower shadow, wind shear using a power law, and spatially coherent turbulence, whereas the hydrodynamic loads were implemented using the Morison equation. Loads and coupled responses were predicted for a set of load cases with different wave headings. An advanced aero-elastic code, Flex5, was extended for the TLP wind turbine configuration, and comparing the response with the simpler model showed generally good agreement, except for the yaw motion. This deviation was found to be a result of missing lateral tower flexibility in the simpler model.

Table 1.2 summarizes the TLPs commissioned worldwide (Chandrasekaran 2017). TLPs have proved their efficiency for deepwater oil exploration in terms of stability and cost-efficiency.

1.3 Guyed Tower and Articulated Tower

Guyed towers are compliant offshore structures whose position restraint is ensured by guy wires. Guyed towers are generally used for small field production and installed up to a water depth of about 500 m. Guy wires limit the lateral motion of the platform deck, while pile and clump weights are used to position the guyed towers on the seabed. Given extreme sea conditions, clump weights are raised from the seafloor, providing an additional restoring force to the tower. Articulated towers are similar to TLPs, with tethers replaced by a single high-buoyancy shell. The buoyant shell offers the required restoring force to counteract encountered lateral loads. The universal joint is a unique component of the tower, which connects it to the foundation system. Depending on the nature of the seabed at the site, the foundation system may consist of a concrete base or a pile foundation. Articulated towers are generally installed at a water depth of about 500 m.

Witz et al. (1986) performed model tests and theoretical studies on rigid semi-submersibles and conducted experimental studies on articulated semisubmersibles. Articulations were placed at the base of the columns and pinned to the vessel base and maintained excess buoyancy over self-weight. Comparison of righting moment curves indicated that the articulated structure showed higher righting

Table 1.2 Tension leg platforms constructed worldwide.

S. no	Platform name	Water depth (m)	Location
		USA	
1	Shenzi	1333	USA
2	Auger	872	USA
3	Matterhorn	869	USA
4	Mars	896	USA
5	Marlin	986	USA
6	Brutus	1036	USA
7	Magnolia	1433	USA
8	Marco Polo	1311	USA
9	Ram Powell	980	USA
10	Prince	454	USA
11	Neptune	1295	USA
12	Ursa	1222	USA
13	Morpeth	518	USA
14	Allegheny	1005	USA
15	Jolliet	542	USA
		Europe	
1	Snorre A	350	Norway
2	Heidrun	351	Norway
		Africa	
1	Okume/Ebano	500	Equatorial Guinea
2	Oveng	280	Equatorial Guinea

moments than the rigid structure. Experimental and analytical results agreed well, while the articulated structure showed lesser responses when compared with the rigid structure. Sellers and Niedzwecki (1992) derived the equation of motion, which was valid for both single- and multi-articulated towers using the Lagrange equation approach. A deepwater tension-restrained articulated tower was studied, and its dimensionless parameters were derived from avoiding resonance excitation given environmental loads. Bar-Avi and Benaroya (1996) presented studies of the response of an offshore articulated tower subjected to deterministic random wave loading. The tower was modeled as an upright rigid pendulum mass concentrated at the top and hinged at the base with Coulomb friction and viscous structural damping. The equation of motion was solved using Borgman's method considering the wave height, wave frequency, buoyancy, drag geometric, and wave force nonlinearities. The wave force was estimated using the modified Morison equation. The PM spectrum was used to generate random waves. Parametric studies were also performed, such as buoyancy, initial condition, wave height, frequency, current velocity, and direction. Based on the studies, it was observed that Coulomb damping reduced the beating phenomenon and RAO.

Nagamani and Ganapathy (2000) studied the dynamic response of a three-legged articulated tower by conducting an experiment and analysis. The legs of the articulated tower were connected to the seabed with universal joints, and the deck and legs were connected with a ball-and-socket joint. It was addressed that the articulated structure should have the stability characteristics of less acceleration in the deck and the smallest possible loading on the articulated joint. The effects of mass distributions on the variations of bending moment and deck acceleration were discussed. Based on the study, it was concluded that the experimental and analytical results compared well, and the bending moments and deck acceleration increased with an increase in wave height. Islam and Ahmad (2003) investigated the relative importance of the seismic response of an articulated offshore tower in comparison to the response due to wave forces. The equation of motion was derived using the Lagrangian approach, and the solution was obtained with the Newmark-beta integration scheme. It included nonlinearities associated with variable submergence, drag force, coulomb damping, variable buoyancy, and added mass, along with the geometrical nonlinearities of the system and the joint occurrence of the waves and seismic forces together with the current given random sea conditions.

1.4 Floating Structures

A floating production system (FPS) is a floating unit that is fully equipped with exploration and production equipment. While in operation, the unit is positioned at the site using either anchors or rotating thrusters. Hydrocarbons explored from the subsea system are subsequently transported to the surface with the help of production risers. FPSs are deployed at water depths ranging from 600 to 2500 m. The FPSO system is a big tanker-type ship that is positioned on the seabed with the help of either anchors or dynamic positioning systems. A FPSO is designed to process and store the oil produced from nearby subsea wells as well. Stored oil is periodically offloaded to a smaller shuttle tanker, which transports the oil to an onshore facility for further processing. A FPSO may be suited for a marginally economic field located in remote deepwater areas where a pipeline infrastructure is not economically feasible.

With further advancements in the process of conceiving more appropriate structural forms to make platforms insensitive to water depth, floating structures have been introduced. A spar platform is a large, deep-draft, cylindrical floating caisson, generally used for exploration and production purposes, and installed at water depths of a few thousand meters. The spar has a long cylindrical shell called a *hard tank*, which is located near the water level. It generates high buoyancy to the structure that helps stabilize the platform; the midsection is annular and used for free flooding. The bottom part is called a *soft tank* and is utilized for placing the fixed ballast. It essentially floats the structure during transport and installation. In order to reduce the weight, drag, and cost of the structure, the midsection is designed to be a truss structure. To reduce the heave response, horizontal plates are introduced between the truss bays. The cell spar is the third generation of spar platforms, which was commissioned in 2004. It has several ring-stiffened tubes that are connected by horizontal and vertical plates. The hull is transported to the offshore site horizontally on its side. At the desired location, the structure is ballasted at the required attitude and then installed. The topside is attached at the site once the installation is complete.

Newman (1963) developed a linearized potential wave theory to estimate the regular wave forces on a spar buoy and presented the response amplitude in the surge, pitch DOF. A spar buoy was modeled separately as an undamped and damped system. Response amplitudes and phase angle plots of damped and undamped systems were discussed. Glanville et al. (1991) analyzed a spar floating drilling production storage structure in the presence of the combined effects of wave, wind, and current loads at a water depth of 800 m. The authors highlighted the stability characteristics, fabrication, and ease of installation of the spar. The equation of motion, which included mass, stiffness, and linearized damping matrices, was solved using a time integration scheme. The results indicated that the spar was cost-effective, insensitive to payloads, and best suited for deepwater drilling and production applications (Agarwal and Jain 2002; Finn et al. 2003; Glanville et al. 1991).

Ran et al. (1996) performed experimental and analytical investigations on a 1 : 55 scale model given regular, bichromatic, and unidirectional irregular waves, with and without sheared currents. Time-domain numerical investigations were performed on the spar in the presence of waves and currents; the wave-structure interaction was modeled considering second-order wave theory, including the effects of viscous and wave-drift damping. Bichromatic and bidirectional wave forces were estimated using second-order diffraction/radiation methods, and the Morison drag formula was used to estimate viscous drag forces. The experimental and numerical results were in good agreement, and the spar responses were within the practically acceptable limits in 100-year-storm sea conditions (Koo et al. 2004). Agarwal and Jain (2002) performed a time-history analysis of a spar platform under wave loads using Airy wave theory, the Morison equation, and the Newmark-beta method considering a spar as a system with six DOF. The spar mode considered the effect of mooring lines connected at fairlead locations. Heave, pitch, and roll stiffness were modeled based on hydrostatics, while the lateral stiffness was modeled using nonlinear horizontal springs. Based on the studies, it was concluded that the inertia and drag coefficients influence the surge and heave responses of the platform (Montasir et al. 2008; Montasir and Kurian 2011).

Finn et al. (2003) performed vortex-induced vibration studies on a cell spar in the presence of waves and current loads in different wave directions. The model was fabricated with different configurations of strakes, and the tests were conducted on the cell spar model, with and without strakes. The model with strakes reported a lower sway response in comparison to that without strakes, and an optimum strake configuration was also suggested. Koo et al. (2004) highlighted the causes of Mathieu instability for a spar due to variable submergence and time-varying metacentric heights in the coupled heave and pitch motions. Effects of the hull, mooring, and riser coupling on the principal instability and damping effects were studied using a modified Mathieu equation, and the effect of wave elevation was also investigated. Based on the simulations, it was concluded that Mathieu instability increased with the increase in pitch motion. Damping was found to suppress the instability, and the additional pitch-restoring moment due to buoyancy also contributed to a reduction in Mathieu instability.

Zhang et al. (2007) performed a numerical simulation on a spar in operating and survival sea conditions. They investigated a cell spar moored with nine mooring lines in a chain-wire-chain form in three groups. Vertical pre-tension in the mooring lines was assumed in the simulation. The Joint North Sea Wave Project (JONSWAP) and Norwegian Petroleum Directorate (NPD) wind spectra were considered and performed in time-domain simulations. Based on the studies, it was concluded that the motions of the spar were found satisfactorily; but the low-frequency motions required care because resonance in heave motions was present in horizontal motions, and second-order drift motions were present in vertical motions. Montasir et al. (2008) performed a dynamic analysis of classic and truss spars in the presence of unidirectional regular and random waves. The spar was considered a rigid body and connected to the sea floor by catenary mooring lines. The water particle kinematics were estimated using Chakrabarti's stretching formula, and wave forces were determined based on the modified Morison equation. Based on a time-history analysis using the Newmark-beta method, the results showed that the spar had better motion characteristics and was economical. Montasir and Kurian (2011) developed a MATLAB code called TRSPAR to analyze a truss spar with strakes in the presence of slowly varying drift forces, and validated it with experimental results. Slowly varying frequency wave forces were derived, and the Morison equation was used for force estimation. The developed code considered various nonlinearities like variable submergence, nonlinear springs for mooring lines, and drag. Neeraj Aggarwal et al. (2015) discussed an offshore wind turbine installed on a spar platform at a water depth of 320 m. The coupled wind and wave analysis was achieved by coupling the FAST aerodynamic software and ANSYS AQWA hydrodynamic software. The power spectral densities of the response were obtained by using the transfer function of the system for irregular sea conditions defined by the Pierson-Moskowitz (PM) spectrum, where the wave parameter was chosen near rough sea conditions ($Hs = 6$ m, $Tp = 10$ s). The Gumbel method shows lower values compared to extremes estimated using the Weibull method. The sensitivity to sample size was also not significant.

As seen from the discussion, offshore structures with different geometric forms are becoming increasingly common and have large displacements under lateral loads. The degree of compliance imposed by their design makes them suitable for deepwater and ultra-deepwater exploration. However, large displacements also make them unsuitable for safe operability. The ideal situation is to have an offshore platform that is highly compliant but does not undergo large displacement under lateral loads, which seems to be entirely hypothetical. However, a few recent studies have attempted to control the large displacements of the deck without compromising their compliancy, as discussed in the following section.

1.5 Response Control Strategies

Recent trends in the geometric design of several structural forms focus on the use of lightweight, highly durable materials. This has increased the probability of the development of structural configurations that are elastic and low damping. A *damper* is a device used to restrain, depress, or reduce the motion of a structure. Dampers are efficient at controlling energy input due to dynamic loading through various mechanisms. The energy gained due to dynamic loading is dissipated through the various mechanisms as either heat or deformation.

Unlike land-based structures, offshore structures under environmental conditions are subjected to secondary vibrations that initiate structural failure, discomfort during topside activities, and breakdown of equipment. Response control methods with passive dampers and base-isolation systems are among the few successful applications on land-based structures but cannot be directly deployed in offshore structures for several reasons. One of the most important and complicated tasks is to tune the frequency of the system vibration to that of the external control devices, such as dampers. Dampers are activated by the motion of the structure and dissipate energy via various mechanisms. Secondary damping devices, which are commonly useful in response control, can be classified into three groups: active, semi-active, and passive systems.

1.5.1 Active Control Algorithm

Active systems, once installed, continuously monitor structural behavior. After processing the information over a short time, they generate a set of forces to modify the current state of the structure. A block diagram of the active control strategy is shown in Figure 1.3. An active control system consists of three major components: (i) the monitoring system, which perceives the present state of the structure and subsequently records the data using an electronic data-acquisition system; (ii) the control system, which determines the reaction forces to be applied to the structure based on the communication received from the monitoring system; and (iii) the actuating system, which applies the physical forces to the structure, as directed by the control system. To accomplish all these things, an active control system needs a continuous external power source. The loss of power that might be experienced during a catastrophic event may render these systems ineffective. A few common examples of this kind are active mass dampers and active liquid dampers.

1.5.2 Semi-Active Control Algorithm

Semi-active systems are similar to active systems except that they need less external power for successful activation. Semi-active control devices are also often viewed as controllable passive devices. Instead of exerting additional forces on the

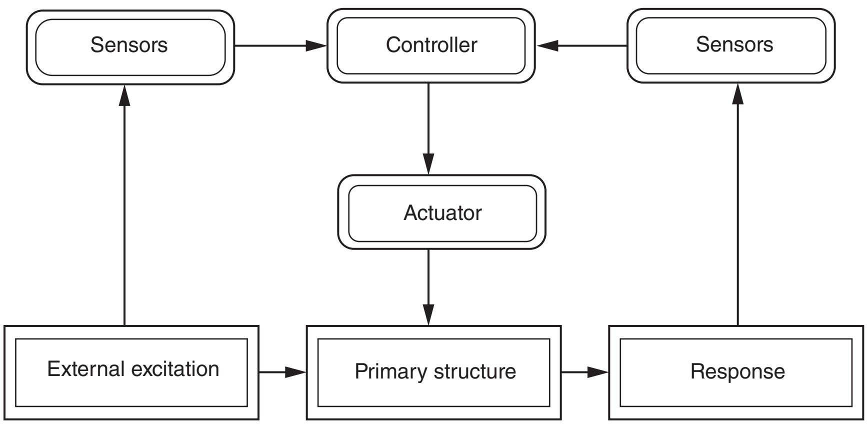

Figure 1.3 Active control strategy.

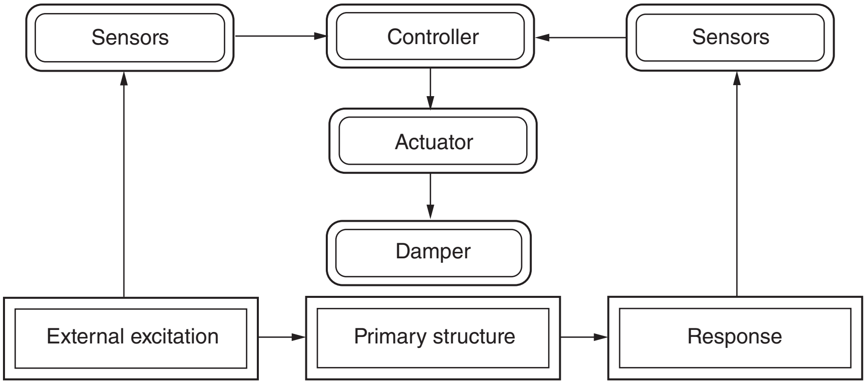

Figure 1.4 Semi-active control strategy.

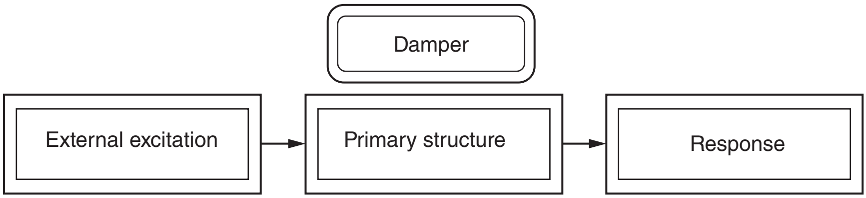

Figure 1.5 Block diagram for passive control strategy.

structural systems, they control vibrations by modifying the structural characteristics. A block diagram representing a semi-active control system is shown in Figure 1.4. The need for an external power source to make these systems functional limits their application in structural engineering, as they may fail due to catastrophic events. Examples of semi-active devices include variable orifice fluid dampers, controllable friction devices, variable stiffness devices, controllable fluid dampers, and magneto-rheological dampers.

1.5.3 Passive Control Algorithm

Passive systems require no external energy for successful operation, which is one of the major advantages of such systems in comparison to the former types. A key benefit of passive control devices is that once installed in a structure, they do not require any startup or operation energy, unlike active and semi-active systems. A block diagram representing a passive control system is shown in Figure 1.5. Passive control devices are active at all times until maintenance, replacement, or dismantling is required. Passive control systems include friction dampers, metallic yield dampers, and viscous fluid dampers. Alternative types of passive control systems contain a spring (or spring-like component), which is tuned to a particular natural frequency of the structure for maximum damping. Examples of these passive control devices are tuned mass dampers (TMDs), tuned liquid dampers (TLDs), and tuned liquid column dampers (TLCDs).

1.5.4 Friction Dampers

Friction dampers are devices installed at the connection of cross-bracing, introduced by Pall in the Canadian Space Agency (Pall et al. 1993). A friction damper consists of two solid bodies that are compressed together. It uses the friction between the two surfaces to dissipate energy. As a structure is subjected to vibration, the two bodies slide against each other, developing friction that dissipates the energy of the motion. These devices have been built into structures and have been successful in providing enhanced seismic protection by being designed to yield during extreme seismic vibration. Wind loads do not provide enough shear force to activate these types of dampers. Figure 1.6 shows a Pall frictional damper.

1.5.5 Metallic Yield Dampers

The typical design for this damper is a triangular or X-shaped plate that absorbs vibrations through the inelastic deformation of the metallic material. These devices are known to have stable hysteretic behavior. They are usually installed in newly built and retrofitted buildings and are successful in reducing seismic loads. Figure 1.7 shows a metallic yield damper.

1.5.6 Viscous Fluid Dampers

Viscous fluid dampers are similar to conventional shock-absorbers. They consist of a closed cylinder-piston, which is filled with fluid (usually silicon oil). The

Figure 1.6 Pall friction damper.

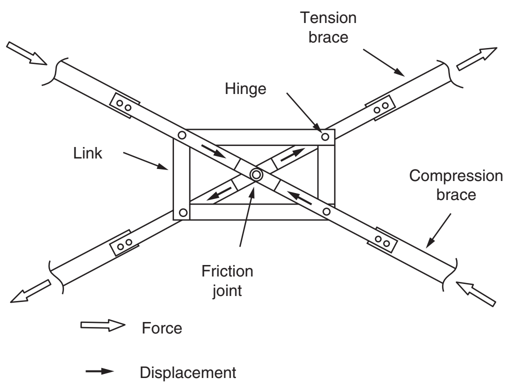

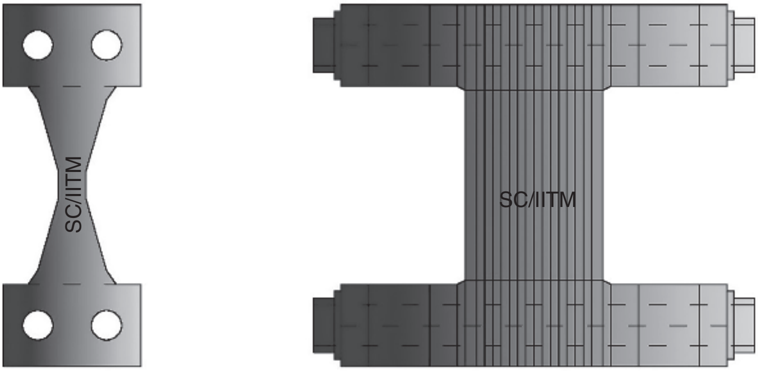

Figure 1.7 Metallic yield damper.

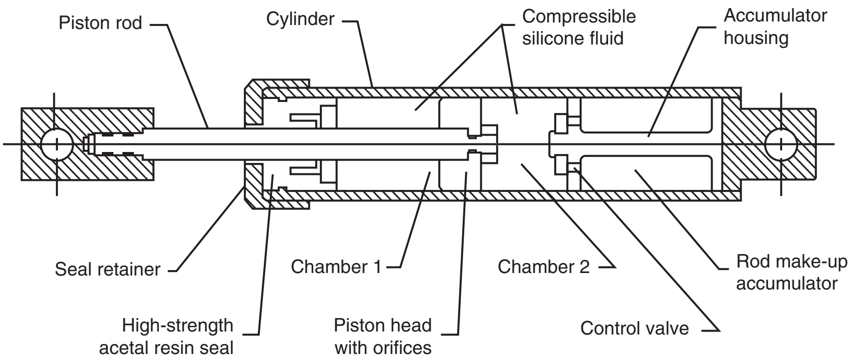

Figure 1.8 Viscous fluid damper.

detailed structural elements of the viscous damper are shown in Figure 1.8. The piston-head contains orifices that regulate the flow of fluid between the two chambers of the piston. When the structure is excited, movement of the fluid through the holes generates friction, and subsequently heat, which dissipates the motion of the structure. These dampers are typically installed as diagonal braces in building frames (preferably steel structures). To provide optimal damping, buildings are often equipped with multiple dampers in place of the diagonal beams on every floor. These viscous dampers have proved to be effective in controlling the vibrations of slender structures under lateral loads (Samuele Infanti et al. 2008).

1.5.7 Tuned Liquid Dampers

TLDs are either rectangular or circular and are installed at the highest floor of a building to control the maximum displacement. Figure 1.9 shows the configurations of TLDs. Depending on the height of the water in the tank, a TLD is categorized as a shallow-water or deepwater TLD (Ahsan Kareem 1990). If the ratio of the height of the liquid column in the damper to the length of the tank (in the case of a rectangular tank) or diameter of the circular tank is lesser than 0.15, then it is classified as a shallow-water TLD (Kareem and Sun 1987). It is important to note that the height of the liquid column in the damper depends on the natural frequency of the structure to be controlled. When the frequency of the tank motion is closer to one of the natural frequencies of the tank fluid, large-amplitude sloshing occurs. Tuning the TLD parameters to the structural parameters induces high sloshing and wave-breaking phenomenon. It helps to dissipate significant energy from the primary structure, resulting in the reduction of structural vibrations.

Ahsan Kareem (1990) suggests a new approach to reduce the building response using TLDs. Structural analyses of the building in response to wind loads were investigated. The boundary layers near the tank walls are assumed to dissipate all the energy. The sloshing in the TLD reduces the structure response by increasing the damping to the system. The vibration of the system is absorbed and dissipated due to wave-breaking and viscous effects. The response reduction by introducing the damper to the structure is effective when the TLD is tuned to the structure frequency. Sun et al. (1995) proposed a nonlinear analytical model of a rectangular tank with a shallow-water TLCD for pitch motion using shallow-water wave theory. The damping of liquid sloshing affects efficiency, and hence it is a significant parameter of the study. The results of the proposed analytical model show a considerable reduction in the resonant pitch response of the primary structure. The effectiveness of mitigating pitch motion depends on the liquid mass in the container, the configuration, and the location of the TLD

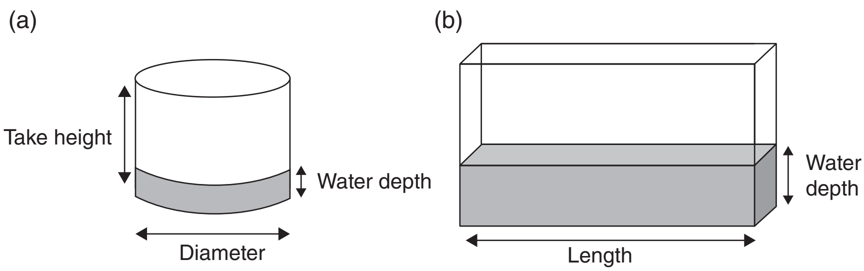

Figure 1.9 Tuned liquid damper: (a) circular; (b) rectangular.

on the structure. Analytical and experimental studies prove that the liquid sloshing in the rectangular tank is nonlinear given a pitching motion. Tait et al. (2008) experimentally investigated the performance of both unidirectional and bidirectional TLDs in response to random excitation. The performance of the TLD was examined under various loads, tuning ratios, and ratios of water depth to tank length. The parametric studies resulted in the development of performance charts, based on shallow-water wave theory, which could help design TLDs for unknown structural frequency.

1.5.8 Tuned Liquid Column Damper

A TLCD is a U-shaped tube half-filled with liquid, as seen in Figure 1.10. Unlike a TLD, which depends on liquid sloshing to dampen structural vibrations, a TLCD controls structural motion by a combined action of the movement of liquid in the tube and the loss of pressure due to the orifice inside the tube (Gao et al. 1997). A nozzle is placed at the horizontal part of the tube. The extent of response control achieved by a TLCD depends on the frequency of the exciting force acting on the structure (Fahim Sadek et al. 1998). While the restoring force is developed by the gravitational force acting on the liquid, the orifice is the controlling element for the dynamics of the liquid sloshing inside the tube. Damping depends on the opening and the type of orifice used.

Balendra et al. (1995) studied the effectiveness of TLCDs for reducing wind-induced motion of towers. The nonlinear equation is linearized to obtain the response of the tower. The Harris spectrum is used to model the along-wind turbulence. The response of the tower is modeled as a SDOF system. By conducting parametric studies, the optimum parameters for a greater response reduction are presented. A similar reduction can be obtained by using a proper opening ratio of the orifice of the TLCD. The opening ratio is varied from 0.5 to 1. It is found that a TLCD with a higher width-to-liquid-length ratio and a high

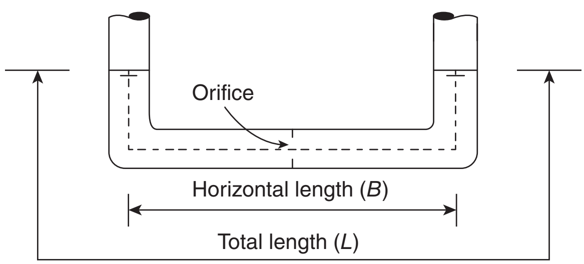

Figure 1.10 Tuned liquid column damper.

mass ratio is better for maximum reduction in acceleration and displacement. For the best response reduction, it is necessary to tune the liquid column damper to the structural frequency. If the TLCD cannot be tuned to the frequency of the structure, satisfactory control can be obtained by choosing a proper opening ratio. Jong Cheng Wu et al. (2005) proposed some useful guidelines for designing a TLCD for a damped SDOF structure. The design table provides the list of necessary optimal parameters and the corresponding response reduction for the design. An empirical formula is proposed for predicting the basic properties of TLCDs and the head-loss coefficient. The optimal tuning ratio and the head-loss coefficient are numerically obtained by minimizing the normalized response of a damped SDOF structure equipped with a TLCD under a white-noise type of wind loading. It is proved that a uniform cross-section is best for a given mass ratio and horizontal length ratio.

Anoushirvan Farshidianfar et al. (2009) studied the vibration behavior of a structure with a TLCD. Using the Lagrange equation, an unsteady and non-uniform flow equation for the TLCD is investigated. By using the normalized mean square value of the nondimensional structure response as the performance index, the analytical formulas of the optimum TLCD parameters for the undamped structure are derived. The tuning frequency ratio, length ratio, and mass ratio are obtained by using the white-noise type of wind excitation, and the performance of the TLCD for controlling the wind-induced responses of a 75-story flexible skyscraper is investigated. For a given length and damping ratio, the optimal value of the tuning frequency ratio is close to 1. Increasing the length ratio can give better control. A mass ratio greater than 3% is impossible to use and does not guarantee good control. A TLCD with a uniform cross-section is recommended for optimum response reduction.

1.6 Tuned Mass Dampers

A TMD is a passive type of damper that imposes response control using the principle of inertia. It applies indirect damping to the structural system. The inertial force of the damper is made to be equal and opposite the excitation force for optimum control. TMDs are used for structures under lateral loads. Figure 1.11 shows a schematic diagram of a TMD. It consists of a secondary mass attached to the main structure through a spring-dashpot arrangement. The energy of the primary structure is dissipated by the inertial force produced by the damper. The damper produces an inertial force in the direction opposite the direction of motion of the structure. The inertial force, in the opposite direction, helps reduce the motion of the primary structure. For maximum response reduction, the parameters of the TMD need to be tuned with

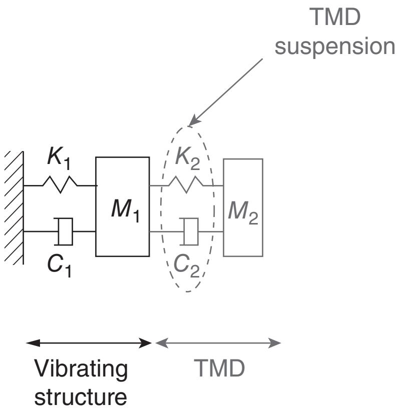

Figure 1.11 Tuned mass damper.

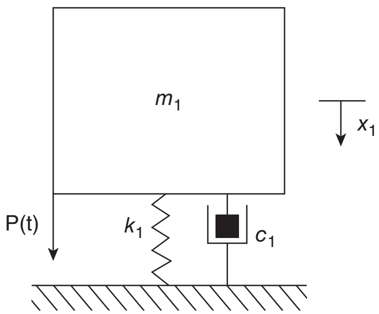

Figure 1.12 Schematic diagram of an idealized system.

those of the primary structure. TMDs are designed to control a single model of a multiple degrees of freedom (MDOF) system (Rana and Soong 1998). Hence, they are tuned to the single structure frequency so that the response in the fundamental mode can be effectively reduced. The addition of a TMD converts a low damping mode in a structure into two coupled higher damping systems with two DOF. The support system for the mass and tuning the frequency are important issues in the design of TMDs. While the mass of the damper is taken as a small fraction of the total mass of the primary structure (usually 1–5%), one of the main limitations is its sensitivity to the narrow frequency band of control. If the TMD is out of tune, its effectiveness is reduced considerably. The primary structure is idealized as a spring-mass SDOF system whose response needs to be controlled (see Figure 1.12). In general, offshore compliant structures exhibit stiff behavior in the vertical plane but remain highly flexible in the horizontal plane. Such behavior offers compliance to the platform without compromising on the payload capacity. The equation of motion of such a SDOF system can be written as:

$$m_1\ddot{x}_1 + c_1\dot{x}_1 + k_1x_1 = P(t) \tag{1.1}$$

Solving this equation of motion will give the displacement of the mass from its equilibrium position. The natural period of the system is given by the following expression:

$$T_n = 2\pi\sqrt{\frac{m_1}{k_1}} \tag{1.2}$$

When a TMD is attached to the structure, the system becomes a two DOF model, as shown in Figure 1.13. An optimally tuned TMD displaces the damper mass to produce a force on the spring in the direction opposite the forcing function; it controls the response of the primary structure. The TMD absorbs energy from the primary system and forces the structure to move in the opposite direction. The equation of motion of the structure with a TMD can be written as:

$$\begin{bmatrix} m_1 & 0 \\ 0 & m_2 \end{bmatrix}\begin{Bmatrix} \ddot{x}_1 \\ \ddot{x}_2 \end{Bmatrix} + \begin{bmatrix} c_1+c_2 & -c_2 \\ -c_2 & c_2 \end{bmatrix}\begin{Bmatrix} \dot{x}_1 \\ \dot{x}_2 \end{Bmatrix} + \begin{bmatrix} k_1+k_2 & -k_2 \\ -k_2 & k_2 \end{bmatrix}\begin{Bmatrix} x_1 \\ x_2 \end{Bmatrix} = \begin{Bmatrix} P(t) \\ 0 \end{Bmatrix} \tag{1.3}$$

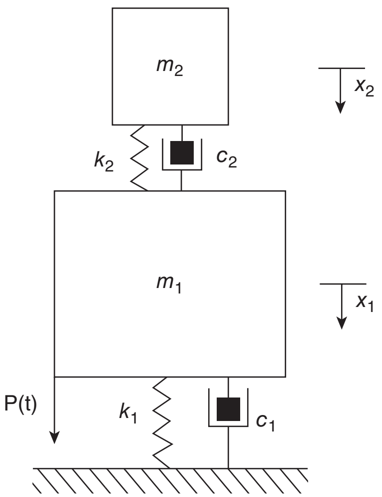

Figure 1.13 Schematic diagram of a spring-mass system with a TMD.

The important parameters that need to be considered in the design of TMDs are the mass ratio and the tuning ratio. While the mass ratio is the ratio of the mass of the damper to that of the primary structure, the tuning ratio is the ratio of the natural frequencies of the damper and the primary structure. The following expressions hold good:

$$T_d = 2\pi\sqrt{\frac{m_2}{k_2}} \tag{1.4}$$

The natural angular frequency of the damper is ω_2:

$$\omega_2 = \frac{2\pi}{T_d} \tag{1.5}$$

$$\text{Mass ratio: } \mu = \frac{m_2}{m_1} \tag{1.6}$$

$$\text{Frequency ratio: } f = \frac{\omega_2}{\omega_1} \tag{1.7}$$

Proper tuning of the mass ratio and frequency ratio of the TMD will produce the maximum response reduction of the primary system. The natural frequency of the damper can be varied by changing the mass and the stiffness of the damper. Ahsan Kareem (1983) studied the parameters of human biodynamic sensitivity to building motion. Various means of controlling the motion of high-rise buildings are discussed. A detailed analysis of a dynamic vibration absorber (TMD) for mitigating objectionable levels of motion of tall buildings is studied. An approximate expression is developed to aid in preliminary design procedures. Fujino and Abe (1993) studied the modal properties of TMD structures with a perturbation technique. The mass of the damper is assumed to be small in the analysis. The efficiency of the mass damper is tested for the non-optimal and optimal parameters of the TMD in response to the harmonic, random, free self-excited motion of the structure. Derived formulas help design the TMD for different types of loading. The formulas are based on the tuning ratio, mass ratio, and damping ratio of the primary structure and TMD. Equations for damping a mistuned TMD are also derived. The derived formulas are very accurate for a mass ratio less than 2%.

Rahul Rana and Soong (1998) did a parametric study on the characteristics of TMDs. The performance of TMDs in response to mistuned TMD parameters are analyzed using the time domain and steady-state harmonic excitations. The time-domain analyses are done based on the El Centro and Mexico excitations. Multi-tuned mass dampers (MTMDs) are used to control multiple structural modes. Detuning of the TMD becomes insignificant when the damping of the structure and the mass ratio are high. It is also found that for structures with high damping, the response reduction caused by the TMD is not significant. Chien Liang Lee et al. (2006) presented an optimal design theory in the frequency domain for the response analysis of structures with TMDs. The optimal damping coefficients and stiffness of the system are determined by reducing the structural response performance index. A numerical scheme is presented to identify the optimal design parameters for multiple TMDs and to facilitate convergence effectively and monotonically. The coupled dynamic system of multiple TMDs with the MDOF structure and the power spectral density function of environment loads are considered in the analysis. The optimal design parameters are systematically determined for minimizing the response in the frequency domain.

Wong (2008) investigated the energy transfer process of using a TMD for an inelastic structure to dissipate earthquake forces. The force analogy method is used to model the inelastic structural behavior. A moment-resisting six-story steel frame is considered for the study. Numerical studies are done to understand the energy transfer and the effectiveness of the TMD on the structure under study. Plastic energy spectra are used to find the effectiveness of the damper at different structural yielding levels. The energy stored in the damper is limited when the structure attains the plastic state. If the efficiency of the TMD is reduced, the structural response is the same as if no TMD is installed on the structure. Studies prove that the installation of a TMD increases the energy dissipation of the primary structure by storing energy. For better efficiency, TMDs can be used to extract plastic energy from the lower levels and subsequently release it at the upper level. Tigli (2012) studied the optimum design of dynamic vibration absorbers (DVAs) installed on linear damped systems under random loads. The study is done for the three cases, minimizing the variance of the displacement, velocity, and acceleration of the main mass. A solution for the optimum absorber frequency ratio is obtained as a function of the optimum absorber damping ratio. The mass ratio of the TMD to the modal mass of the building mode responsible for the significant portion of the response is selected to be 0.03 due to practical limitations. From the simulations, it is found that the optimum absorber damping ratio is not significantly related to structural damping. Approximate closed-form optimum design parameters were proposed when the displacement and acceleration variances were minimized. The main advantage of the method is that all the response parameters can be minimized simultaneously.

Viet and Nghi (2014) suggest a nonlinear, single-mass, two-frequency pendulum TMD to reduce horizontal vibration. The proposed TMD contains one mass moving along a bar; the bar can rotate around the fulcrum point attached to the controlled structure. In response to a horizontal excitation, the single TMD mass has two motions (swing and translation) at the same time, and the proposed TMD has two natural frequencies. The nonlinearity of the pendulum is used to increase the number of DOF of the TMD. An approximated solution for the system is provided by solving a scalar algebraic equation. The natural frequencies of the swing and translation motions, respectively, should be tuned to be near the structure frequency and twice the structure frequency.

1.7 Response Control of Offshore Structures

Dong Sheng et al. (2002) experimentally studied the effectiveness of TLDs in reducing the dynamic response of a fixed offshore structure under wave loading. Rectangular and circular TLDs of different shapes and sizes with different water depths are examined. The number of parameters, such as container shape, size, wave characteristics, frequency ratio, and mass ratio, is considered. For maximum reduction of structural response, the frequency ratio should be near to unity. The results showed that three small circular dampers are more effective than a single large circular damper at a low frequency. However, a single large damper is suitable for a higher frequency. As the wave height increases, the reduction in response also increases. When the incident wave period is near twice the fundamental structure period, the maximum reduction is obtained. The response of the structure can be reduced for a wide range of frequencies. It is suggested that this type of damper could be used for fixed offshore structures in the presence of random waves.

Lee et al. (2006) studied the response reduction of a floating platform attached to a TLCD given wave-induced vibrations. The stochastic analytical method in the frequency domain is utilized, and due to this, the linearization scheme for the system is applied. The Morison equation for a small body is used to calculate the wave forces. Parametric studies are done for the draft and size of the pontoons. A model test is conducted to check the feasibility of the TLCD device applied to the platform. It is found that a perfectly tuned TLCD reduces the response at the resonant frequency. Analytical results show that the energy dissipated from the TLCD device on the floating platform system may be from 50 to 70%. The draft and dimensions of the platform influence the performance of the TLCD. The mass variation does not have much effect on the performance of the TLCD. Qiao Jin et al. (2007) studied the efficiency of circular TLDs on reducing the seismic response of a jacket structure with a liquid sloshing experiment, a model experiment, and numerical analysis. A numerical investigation is carried out using the lumped mass method. A higher mass ratio of the TLD is very efficient for reducing the response of the platform under earthquake loading. TLDs are found to be effective for a mass ratio from 0.01 to 0.05.

Taflanidis (2008, 2009) proposed a robust stochastic design approach for appropriate tuning of the TMD. A TLP having a different natural period for the pitch and heave motions is considered for the study given random sea conditions. The application of two mass dampers is suggested for efficient reduction of pitch and heave motions. TMDs modeled as secondary masses are connected to the hull of the TLP with the help of a dashpot and springs. The study is done to understand the effect of a single damper and two dampers attached to the hull to increase the safety of the platform. The results showed that the use of two dampers in parallel operation was effective in the response control of heave and pitch motions. Colwell and Basu (2009) did simulation studies on the structural response of an offshore wind turbine attached to a TLCD. Environmental loading is considered by combining the wind loads from the Kaimal spectrum and the wave loads from the JONSWAP spectrum. Numerical simulation is carried out, modeling the turbine tower as a MDOF system. Blades at the stationary position and rotating condition were investigated. The system with a TLCD showed reduced bending moment and displacement. The peak response is reduced by 55%. Also, the fatigue life of the wind turbine is enhanced.

Chandrasekaran et al. (2010) studied dynamic response characteristics such as bending stress variations and the displacement of a multi-legged articulated tower (MLAT) through experiments. A TMD is attached to the bottom of the deck plate. Its natural frequency is tuned near to the natural frequency of the MLAT vibration mode that is to be controlled. The MLAT itself is modeled as a SDOF mass-spring-damper system. A significant reduction in the bending moment of the tower is observed for higher wave heights. The maximum reduction is observed at a near-resonant frequency of the structure. Lee and Juang (2012) proposed a new concept of an underwater tuned liquid column damper system (UWTLCD). The study focused on increasing structural integrity by reducing the response of the structure to the incident wave and stresses on the structure. A TLCD with smaller horizontal tubes is pooled into the pontoon of the TLP. Experimental studies were done to find the effectiveness of the UWTLCD in reducing the response. A parametric study was conducted on the effect of wave conditions, the height of the pontoon, and the liquid-length of the TLCD. The results prove that a properly tuned UWTLCD system is very effective at reducing the hydrodynamic response and the tensile force on the tethers. It is shown that a UWTLCD can effectively reduce the heave response.

Moharrami and Tootkaboni (2014) proposed an innovative concept for reducing the displacement response of a tower fixed offshore platform to wave loads. A hydrodynamic buoyant mass damper (HBMD) uses the damper's buoyancy and inertial forces along with hydrodynamic damping effects to reduce the displacement response of the platform. A jacket fixed platform is investigated in which the HBMD is added at the appropriate elevation. As a result of the damper's eccentricity for the platform's position in its deformed configuration, the upward buoyancy force causes a reversal moment that can potentially counteract forces generated by wave loads. The HBMD moves through a surrounding fluid and creates reversal forces on the structure, which moderate those from the wave loads. The reversal forces consist mainly of the inertial force and the buoyancy force. In addition to inertia and buoyancy forces, forces associated with eddy formations in the proximity of the HBMD also help to reduce the platform's response under wave loading.

1.8 Response Control of TLPs Using TMDs: Experimental Investigations

Experimental studies on response control of a TLP in the presence of a TMD are discussed (Ranjani 2015; Chandrasekaran et al. 2016). A scale TLP model is fabricated at a 1 : 100 scale ratio using Froude scaling to include the effect of gravity forces and wave resistance in the model. Experiments are carried out for three different cases: (i) TLP model without a TMD (Case 1), (ii) TLP model with a TMD of mass ratio 1.5% attached to the structure (Case 2), and (iii) TLP model with a TMD of mass ratio 3.0% attached to the structure (Case 3). They are examined in the presence of both regular and random waves. The geometric sizing of members and the plan dimensions of the assumed model are derived from the Auger TLP, Gulf of Mexico. Acrylic material is used to fabricate four columns of 250 mm outer diameter and 5 mm thickness; the height of the column is 490 mm. The bottom and top of the column members are closed with an acrylic sheet of 10 mm thickness. An additional sheet of 10 mm thickness is placed inside each column to provide the required lateral stiffness for the members. The spacing between the longitudinal columns is 850 mm, while the spacing between the transverse columns is 650 mm. Pontoons of the rectangular cross-section of size 90×110 mm are used in the model. The deck of the TLP is made of a 1000 mm square acrylic sheet of 5 mm thickness. Clearance between the column and deck is fixed at 25 mm, and a draft of 300 mm is maintained.

The TMD considered in this experiment consists of a solid mass and a spring element. The mass is fabricated from 10 mm thick acrylic sheets. A rectangular 120 mm $\times$ 100 mm $\times$ 850 mm box is fabricated, as shown in Figure 1.14. The mass of the rectangular box is 0.6 kg ($\mu = 1.5\%$). A mass ratio of 3% is achieved by adding 0.6 kg of sand to the box. To ensure free movement of the attached secondary mass, frictionless rollers 40 mm in diameter are attached to the base plate of the box with a clearance of 15 mm. Two sides of the box are fixed with a ring arrangement for attaching the spring, as shown in the figure. The spring is made of steel wire 1 mm in diameter. A hook is formed at both ends of the spring to connect the mass. The spring is fabricated with a constant outer diameter of 50 mm for both models, as shown in the figure. Several active coils are chosen with 30 and 15

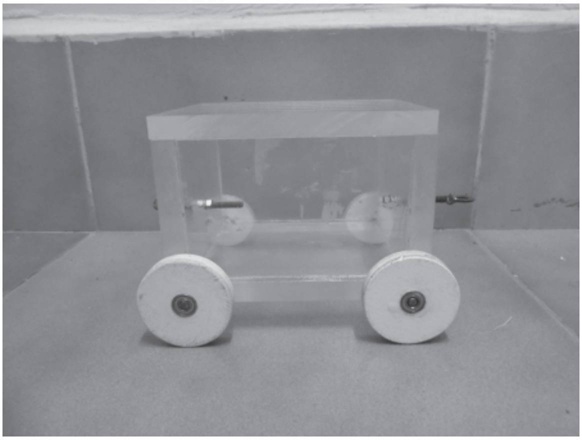

Figure 1.14 Mass used in the TMD.

Table 1.3 Properties of a TMD in the model and prototype (scale 1 : 100).

	Model		Prototype	
Description	**Case 2**	**Case 3**	**Case 2**	**Case 3**
Mass of damper	0.6 kg	1.2 kg	600 T	1200 T
Outer diameter of spring	50 mm	50 mm	5 m	5 m
No. of active coils	30	15	30	15
Pitch (mm)	0.5 mm	0.5 mm	0.05 m	0.05 m
Stiffness of spring	2.76 N/m	5.87 N/m	27.6 kN/m	58.7 kN/m

turns to suit the required mass ratios of 1.5% and 3.0%, respectively. The model details of the TMD are given in Table 1.3.

The model tests are conducted in the presence of regular waves with a wave height of 4, 8, and 12 cm, at a wave heading angle of 0° in a period ranging from 1.2 to 4.4 seconds with a time interval of 0.2 seconds. There was sufficient waiting time between each test to achieve calm water conditions. Experimental investigations are also carried out with random waves of significant wave height (8 cm) and a period ranging from 1.2 to 3.25 seconds. The PM spectrum is used to obtain random sea conditions, given by the following expression:

$$S(\omega) = 5\pi^4 \frac{H_s^2}{T_p^4} \frac{1}{\omega^5} exp\left(-\frac{20\pi^4}{T_p^4} \cdot \frac{1}{\omega^4}\right) \tag{1.8}$$

Table 1.4 Results of free oscillation tests of the TLP model.

	TLP surge		**Pitch**		**TMD surge**		**Difference %**	
	T_n (s)	**ζ (%)**	**T_n (s)**	**ζ (%)**	**T_n (s)**	**ζ (%)**	**T_n (s)**	**ζ (%)**
TLP without damper	4.02	9.97	0.5	35.69	—	—	—	—
TLP with damper (μ = 1.5%)	4.2	13.65	0.46	35.98	2.2	8.98	4.47	36.9
TLP with damper (μ = 3.0%)	4.4	16.69	0.45	36.25	2.2	12.10	9.45	67.4

The time history of the wave height, surge, heave responses, and variation in tether tension are recorded simultaneously for a period of about 60 seconds. Table 1.4 shows the results of free-oscillation tests, with and without dampers.

It can be seen that the presence of the damper increases the surge period and damping ratio for the chosen mass ratios. When the TMD is attached to the TLP, the mass of the TLP increases for the chosen mass ratio. It results in an increase in the period of the platform in the presence of the TMD. The surge period increases up to 4.47 and 9.45% for the two different mass ratios under consideration. It is observed that the damping ratio of the structure increases by 36.9 and 67.4% in the surge. However, the presence of the TMD does not significantly influence the natural period and the damping ratio of the structure in the stiff DOF (for example, pitch). The inertial force generated by the TMD controls the response of the platform. Maximum response control is expected when the responses of the platform and TMD are out of phase with each other. Figures 1.15 and 1.16 show the surge-displacement time history of both the platform and the TMD for two different mass ratios with a wave height of 12 cm and a period of 1.2 seconds. It is seen that the response of the TMD is out of phase with the structure response, which is necessary to achieve effective control.

It is known that the response of the TMD will increase with the increase in the period of the damper, which may result in a larger displacement of the TMD beyond the deck space. Figure 1.17 shows the surge RAO of the TMD for different mass ratios. At lower wave periods, the response of the TLP is much less, and the TMD does not get enough energy to become active. Hence the response of the TMD is also much less. As the wave period increases, the response of the TLP increases, which excites the TMD to come into operation. The response of the TMD increases until it reaches its natural period. Since the response of the TMD is restricted, it was observed that from the natural period of the TMD, the TMD had a response until the maximum possible limit. Hence a constant response is obtained.

Response control of a TLP with a TMD is also examined in the presence of random waves. A comparison of the surge acceleration spectrum for a TLP with and

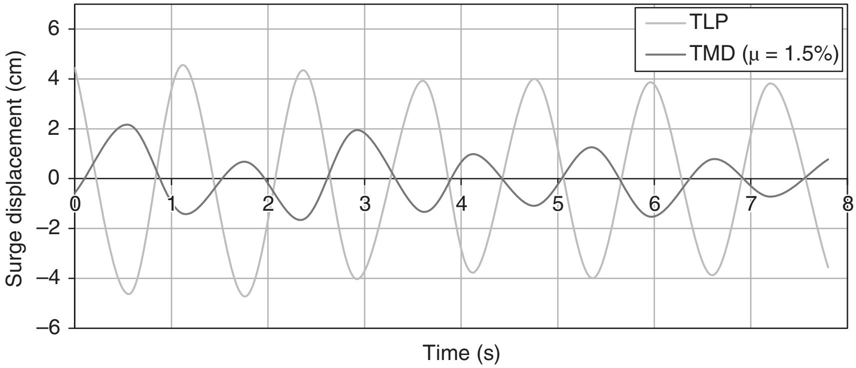

Figure 1.15 Response of a TLP and TMD (μ = 1.5%).

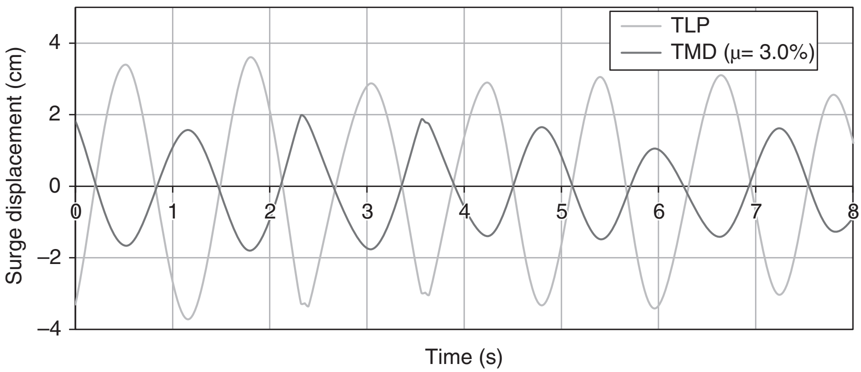

Figure 1.16 Response of a TLP and TMD (μ = 3.0%).

without a damper for a significant wave height of 8 m at various peak periods is shown in Figures 1.18–1.21. The peak surge response is observed near the peak period of the excitation wave. It is also seen that the addition of a TMD reduces the peak amplitude of the surge response considerably. The root mean square (RMS) values of the surge response of the TLP with and without a damper in response to various random excitations are summarized in Table 1.5.

A comparison of pitch response with and without a damper for a significant wave height of 8 m at various periods is shown in Figures 1.22–1.25. It is seen from the figures that the peak response is observed near the peak period of the excitation wave, while the presence of a TMD causes a significant reduction in peak amplitude of the response. The increase in mass ratio reduces not only the peak amplitude but also the overall response of the TLP. The RMS values of the pitch

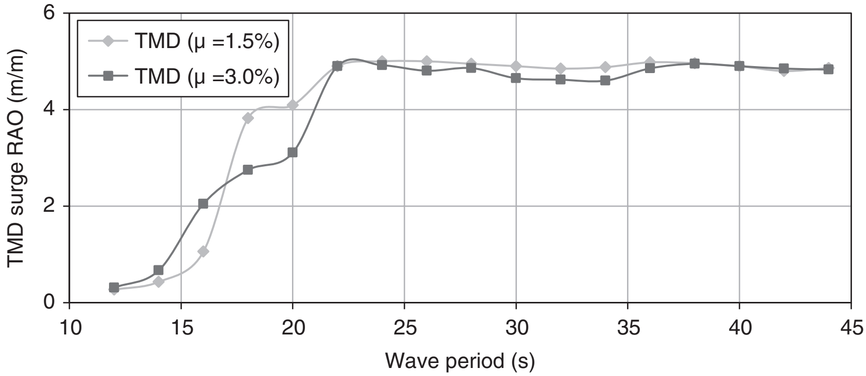

Figure 1.17 Surge RAO of a TMD.

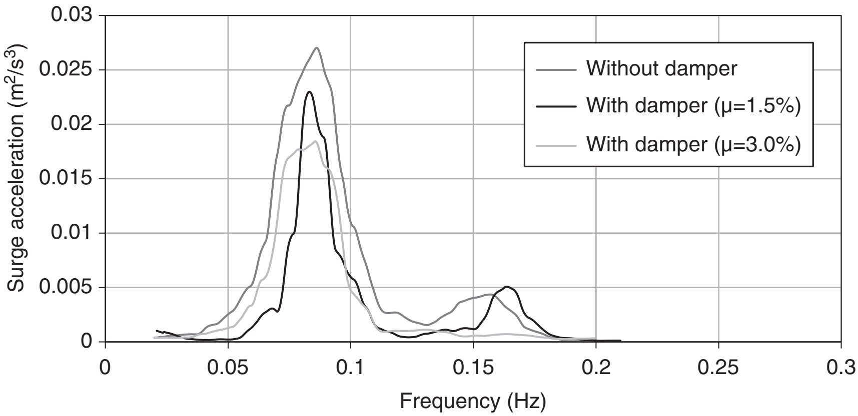

Figure 1.18 Comparison of surge response (H_S = 8 m; T_P = 12 seconds).

response with and without a damper in response to various random excitations are summarized in Table 1.6.

The TLP produces a higher response at longer wave periods and increased wave heights. This response needs to be controlled, which can be achieved by using a TMD with a higher mass ratio. It is also evident that considerable energy is available with higher amplitude waves to activate the TMD motion. Experimental investigations carried out on the scale model of a TLP in the presence of a TMD confirmed the following:

i) A spring-mass system with a higher mass ratio is effective for response reduction with a wide range of periods.
ii) A TMD shows better control for larger wave heights.

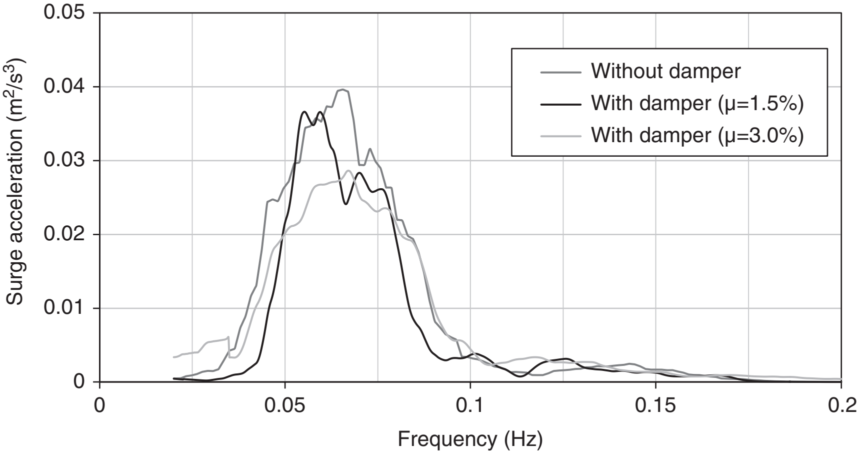

Figure 1.19 Comparison of surge response (H_S = 8 m; T_P = 16 seconds).

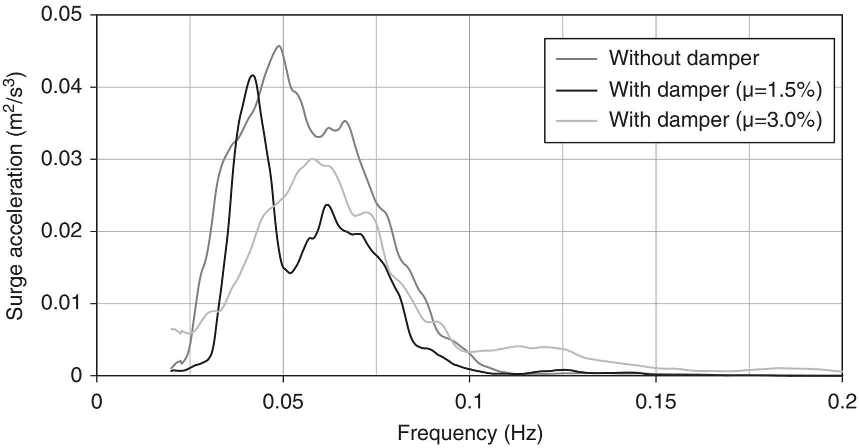

Figure 1.20 Comparison of surge response (H_S = 8 m; T_P = 20 seconds).

iii) An increase in wave elevation increases the surge response at higher periods.
iv) Adding a TMD to the structure shifts the surge, heave, and pitch natural periods and increases the damping ratio of the structure.
v) The response reduction is found to be high for higher mass ratios. Maximum response reduction, up to 10.9 and 16%, is obtained mass ratios of 1.5 and 3.0%, respectively.
vi) Greater heave response reduction is observed due to the reduction of the surge response and tether tension variation. A maximum reduction of 19 and 28% is obtained in the heave response for mass ratios of 1.5 and 3.0%, respectively.

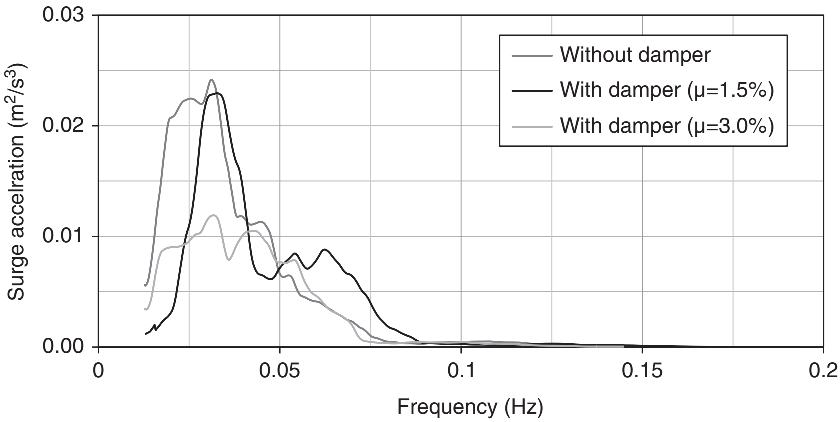

Figure 1.21 Comparison of surge response (H_S = 8 m; T_P = 32.5 seconds).

Table 1.5 RMS value of surge responses in the presence of random waves.

Period	TLP without damper	TLP with damper (1.5%)	TLP with damper (3.0%)	Response reduction % (μ = 1.5%)	Response reduction % (μ = 3.0%)
12	0.104	0.095	0.087	8.6	16.6
16	0.126	0.117	0.103	7.5	18.5
20	0.140	0.130	0.119	7.2	15.1
32.5	0.155	0.146	0.135	5.9	12.9

vii) By controlling the surge response, indirect control of the heave and pitch DOF is achieved. A maximum reduction of 13 and 16% is obtained in pitch for mass ratios of 1.5 and 3.0%, respectively.

1.9 Articulated Towers

Articulated towers are semi-compliant offshore structures consisting of a universal joint that connects the tower to the seabed. The presence of a universal joint allows the structure to move and thereby reduces the forces acting on the tower. The articulated tower (AT) has emerged as one of the most reliable systems for single-point mooring, control towers, and flare structures but can also be used as a production platform for marginal fields, or as a processing unit in remote, hostile environments. This kind of platform can be seen as an extension of the TLP in

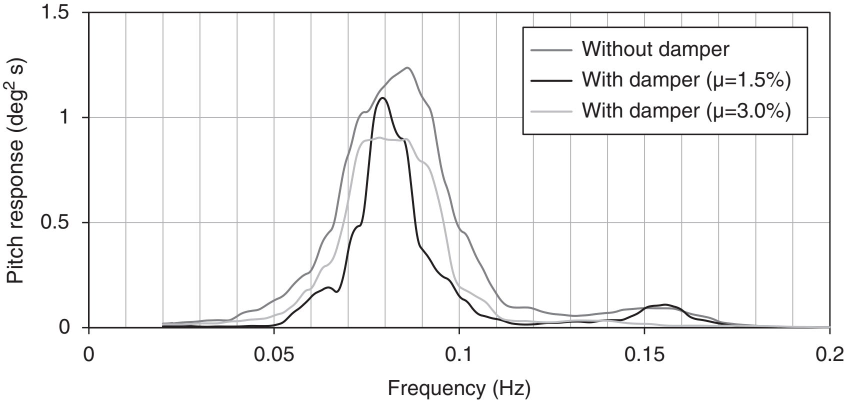

Figure 1.22 Comparison of pitch response (H_S = 8 m; T_P = 12 seconds).

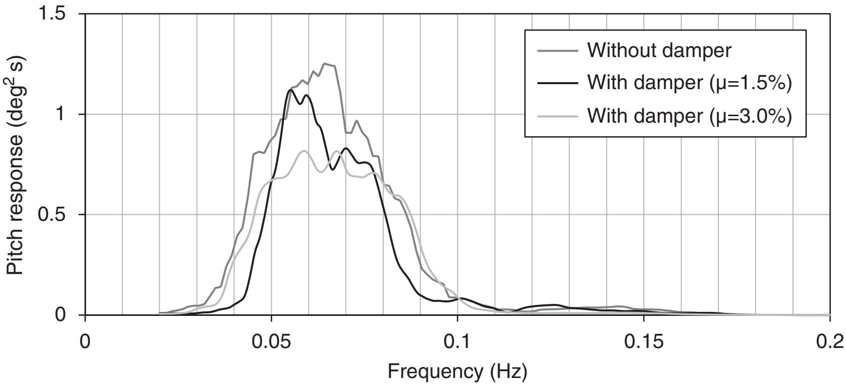

Figure 1.23 Comparison of pitch response (H_S = 8 m; T_P = 16 seconds).

which the tension cables are replaced by one single buoyant shell with sufficient buoyancy to produce required restoring moment against lateral loads. An articulated tower is then flexibly connected to the seabed through a universal joint and held vertically by the buoyancy force acting on it. Similar to a reed that "bends but does not break," the suppleness of articulated structures withstands the combined effects of wind and waves. As the connection to the seabed is through the articulation, the structure is free to oscillate in all directions and does not transfer any bending moment to the base.

The first AT was built and operated in the Argyll Field in the North Sea in 1975. The basic configuration of an AT is shown in Figure 1.26. It comprises five cylindrical subsections erected consecutively in the vertical plane: the connector at the lower part, ballast chamber, lower shaft, buoyancy chamber, and upper shaft. The

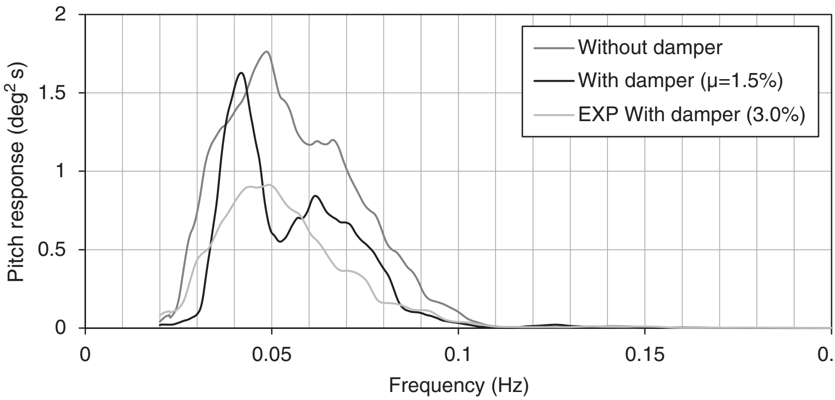

Figure 1.24 Comparison of pitch response (H_S = 8 m; T_P = 20 seconds).

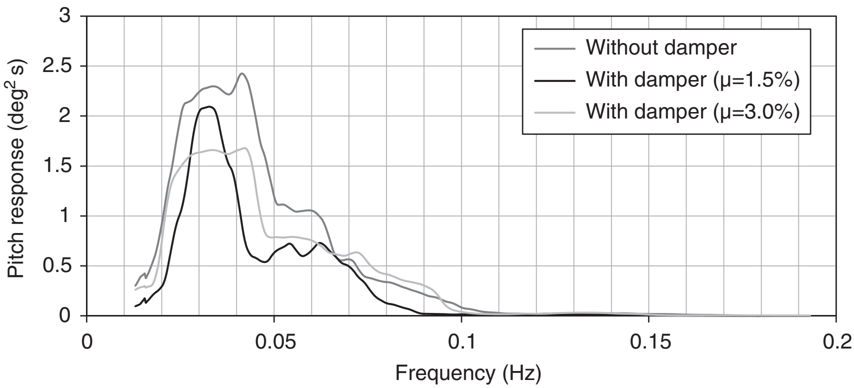

Figure 1.25 Comparison of pitch response (H_S = 8 m; T_P = 32.5 seconds).

connector is joined to the base at the sea bottom and called a *universal joint*, while the upper shaft supports a deck structure where necessary topside facilities are accommodated. Unlike fixed structures, which are designed to withstand environmental forces without substantial displacement, ATs are designed to allow small but not negligible deformation and deflection that are made possible by the presence of the universal joint. The utilization of the universal joint also relieves the foundation from resisting any lateral force developed by environmental action.

One of the primary features of an AT is its ability to displace from its initial position when subjected to environmental loads, hence reducing the maximum internal response of its structural elements. Under environmental loads, the AT displaces in the rotational mode of the universal joint located on the base. A large buoyancy chamber enables recentering of the tower, once displaced. The buoyancy chamber

Table 1.6 RMS value of pitch responses in the presence of random waves.

Period	TLP without damper	TLP with damper (1.5%)	TLP with damper (3.0%)	Response reduction % (μ = 1.5%)	Response reduction % (μ = 3.0%)
12	0.683	0.604	0.546	11.5	20.0
16	0.695	0.597	0.537	14.1	22.7
20	0.840	0.755	0.690	10.2	17.9
32.5	0.962	0.848	0.776	11.8	19.4

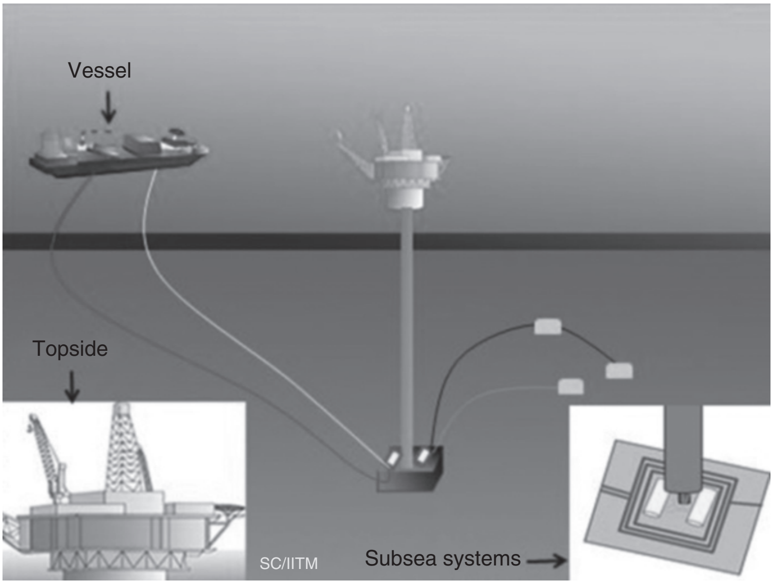

Figure 1.26 Articulated tower. *Source:* Chandrasekaran 2017.

is considered the most important element, since it provides essential stiffness to the system through buoyancy-restoring forces. In a typical AT, when a moored tanker pulls the top of the tower to one side, tilting the tower, the buoyancy compartment moves as an arc about the pivot pint to recenter the tower. However, in shallow water, a small angle of tilt of the tower results in a decreasing moment arm, which proportionately decreases the restoration force. It can be compensated for by utilizing a larger buoyancy compartment, but this results in a large, costly system. The use of a buoyancy chamber in place of guy lines or a tether is required to restrain any possible excessive motions, thus simplifying the system even further.

ATs are considered economically attractive in deepwater applications due to their reduced structural weight and simplicity of fabrication, compared to other conventional platforms. They are well suited for water depths ranging from 150 to 500 m. One advantage of this type of system over those that utilize a freely floating buoy held by catenary chains is the fact that fluid-carrying conduits can be placed to extend through the rigid tower to protect these conduits. Another advantage is that the tower can extend high above the water to provide an attachment point for a hawser connected to a ship, without destabilizing the system. As the water depth increases, it is preferable to add another universal joint along the height of the tower. An AT with universal joints in the intermediate level is called a single-leg multi-hinged AT. The extension of the concept of the single-leg AT led to the development of a new type of platform with several columns that are parallel to one another: the MLAT.

A MLAT is an AT in which, instead of a single shell, the deck is attached to the seabed by three or four legs that are parallel to one another and connected by universal joints both to the deck and to the foundation. The use of universal joints ensures that the columns always remain parallel to one another and the deck remains in a horizontal position. There is no rotation about the vertical axis of the columns. The advantage of this system is that the payloads and deck areas can be increased. Further, they are comparable to conventional production platforms in moderate water depths; and the sway or horizontal displacement of the deck is considerably reduced compared to single-leg ATs, making the use of such platforms feasible even as production units in deep water or ultra-deep water. In this sense, it is important to reduce the displacement of the superstructure as much as possible. This can then enable the installation of more facilities that are needed for production, and also ensure save living units on the topside. One of the drawbacks is that while for a single- or multi-hinged AT, the high period generally avoids resonance problems, these structures are characterized by closer periods of waves (occurring every 10–20 seconds) and could be subjected to resonance problems. Under such conditions, the platforms' safe operability needs to be guaranteed through effective design; but the literature is still poor, offering no feasible solution until now.

1.10 Response Control of ATs: Analytical Studies

A system on which a steady alternating force of constant frequency is acting may result in undesired vibrations, especially when the excitation frequency is close to the structure's fundamental frequency. In order to solve this problem, one may try to eliminate the force bandwidth. One can also attempt to change the structural characteristics of the system. However, in the case of offshore structures, the latter option influences the buoyancy of the system. An alternative solution to reduce the undesired vibration response is to apply a kind of DVA to the system, such as a TMD. The TMD chosen for the current application is a pendulum, as this is a simple and efficient tool to control the response. The MLAT is modeled as a SDOF mass-spring-damper system on which is attached the TMD, which consists of a comparatively small vibratory system k_2, m_2, attached to the main mass m_1. Such a system is represented schematically in Figure 1.27.

The equation of motion governing this system is given by:

$$\begin{cases} m_1\ddot{x}_1 + c_1\dot{x}_1 + k_1x_1 + c_2\left(\dot{x}_1 - \dot{x}_2\right) + k_2\left(x_1 - x_2\right) = P_0\sin\omega t \\ m_2\dot{x}_2 + c_2\left(\dot{x}_2 - \dot{x}_1\right) + k_2\left(x_2 - x_1\right) = 0 \end{cases} \tag{1.9}$$

in which both x_1 and x_2 are harmonic motions of the frequency (ω) and can be represented as vectors. The easiest manner of solving this system is to write these vectors as complex numbers. The steady-state solution is represented by the following equation:

$$\begin{cases} x_1e^{j\omega t} \\ x_2e^{j\omega t} \end{cases} \tag{1.10}$$

Figure 1.27 Analytical model.

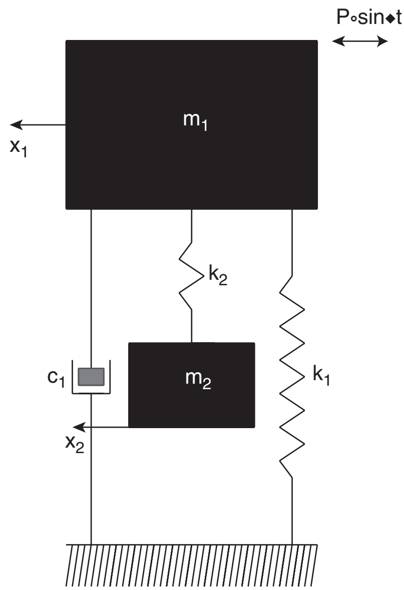

where x_1 and x_2 are complex numbers. Differentiating these solutions, substituting them in Eq. (1.9), and dividing for $e^{j\omega t}$ transforms the differential into the algebraic equation show here:

$$\begin{cases} (-m_1\omega^2 + c_1 j\omega + k_1 + k_2)x_1 - k_2 x_2 = P_0 \\ (-m_2\omega^2 + k_2)x_2 - k_2 x_1 = 0 \end{cases} \tag{1.11}$$

Solving for x_1, we get:

$$\left(\frac{x_1}{P_0}\right)^2 = \frac{(-m_2\omega^2 + k_2)^2}{\left[\left(-m_1\omega^2 + k_1\right)\left(-m_2\omega^2 + k_2\right) - k_2 m_2 \omega^2\right]^2 + c_1^2\omega^2\left(-m_2\omega^2 + k_2\right)^2} \tag{1.12}$$

from which one can see that x_1 is a function of seven variables: P_0, ω, c_1, k_1, k_2, m_1, and m_2. For simplification, we can put this equation in a dimensionless form by introducing the following symbols:

$$x_{st} = P_0 / k_1$$

$$\omega_a{}^2 = k_2 / m_2$$

$$\Omega_n{}^2 = k_1 / m_2$$

$$\mu = m_2 / m_1$$

$$f = \omega_a / \Omega_n$$

$$g = \omega / \Omega_n$$

$$c_c = 2m\omega_a$$

where x_{st} is the static deflection of the main system, $\omega_a{}^2$ is the natural frequency of the absorber, $\Omega_n{}^2$ is the natural frequency of the main system, μ is the mass ratio, f is the natural frequency ratio, g is the forced frequency ratio, and c_c is the critical damping. After simplifications, Eq. (1.12) reduces to the following simple form:

$$\frac{x_1}{x_{st}} = \sqrt{\frac{(-f^2 + g^2)^2}{\left[\left(-g^2 + 1\right)\left(-f^2 + g^2\right) - \mu f^2 g^2\right]^2 + 4\frac{c_1{}^2}{c_c{}^2} g^2 f^2 \left(-\mu f^2 + \mu g^2\right)^2}} \tag{1.13}$$

It can be seen that this equation expresses the amplitude ratio in terms of four essential variables instead of seven: μ, c_c, f_2, and g_2. This simplified form of the response of the primary system exhibits a variation, as shown in Figure 1.28 for a

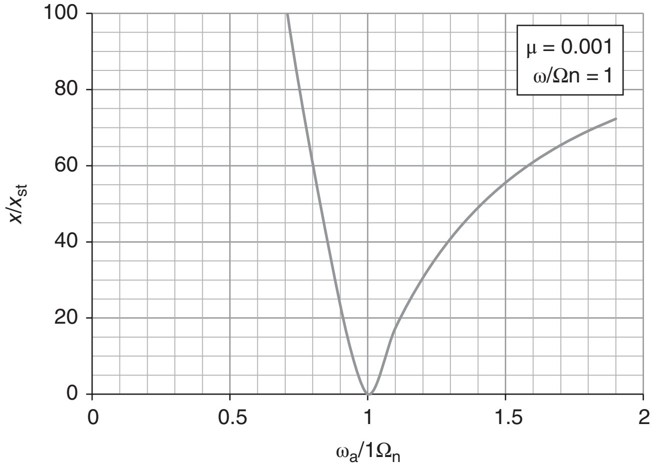

Figure 1.28 Variation of responses for different frequency ratios.

mass ratio of 0.1% and a frequency ratio of unity. We can see that the range of the absorber frequency is narrow for an effective reduction of displacement.

However, by considering a secondary mass as a TMD, the variation of response of the primary structure with a TMD of the same frequency based on the action of waves can be controlled. Figure 1.29 shows the variation of response for different frequency ratios with a TMD. It is seen that such a system can avoid displacement at the resonance frequency. This is due to the fact that the inertial force of the TMD, at all instants, acts opposite in phase with the excitation force P_o sin ωt. It results is no force acting on the main system and hence does not vibrate the primary system at all. Moreover, this also shows that the presence of a TMD can reduce displacement even when the excitation frequency is smaller than the structural frequency. Hence, for structural systems subjected to a variable frequency excitation, as in the present case, the addition of a TMD can result in additional problems because it generates two resonant peaks instead of one. However, interestingly, response build-up, even given these near-resonance conditions, can be controlled by introducing a damper in the TMD (Den Hartog 1985).

The influence of the mass ratio in the system is shown in Figure 1.30. It is evident that the increase in mass ratio increases the response reduction significantly for the same frequency ratio of unity. Unfortunately, this is not a feasible solution for offshore structures as an increase in mass affects buoyancy and thereby stability. Hence, beyond a threshold value, it is not possible to control the response using a TMD. In the following section, experimental investigations carried out on response reduction of an AT using a TMD are discussed.

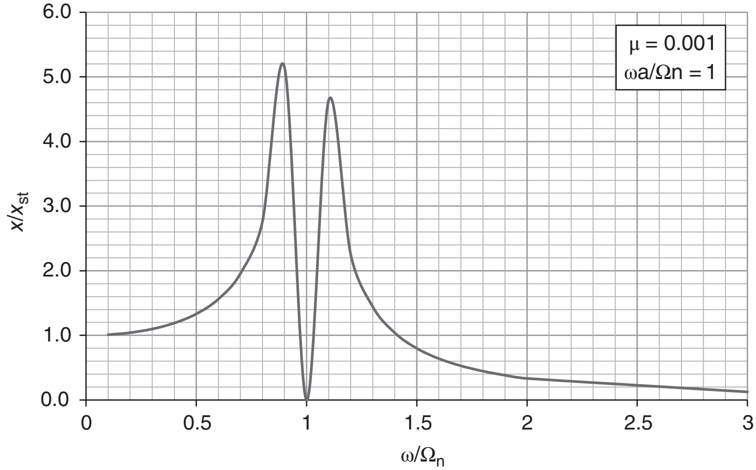

Figure 1.29 Variation of responses for different frequency ratios with a TMD.

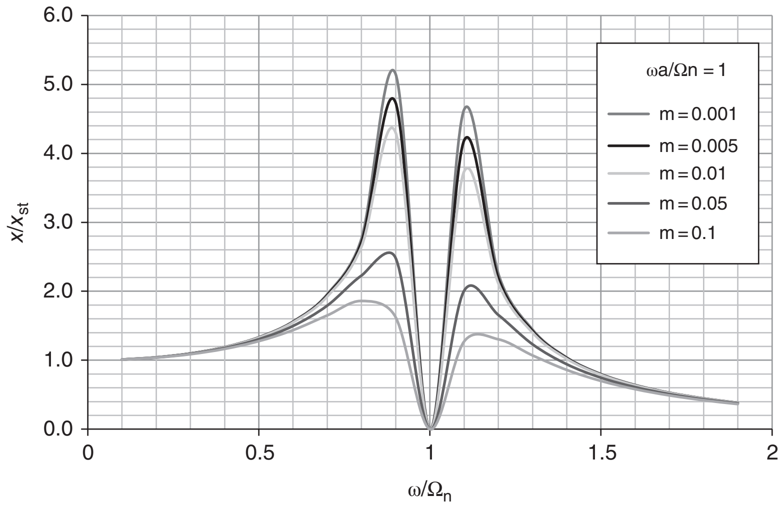

Figure 1.30 Variation of responses for different frequency and mass ratios with a TMD.

1.11 Response Control of ATs: Experimental Studies

A scale model of a MLAT is fabricated to a scale of 1 : 100. Perspex is used to fabricate the model and ensure that during test conditions, stresses that develop in the members do not exceed the elastic limit of the chosen material. The mechanical characteristics of Perspex are summarized in Table 1.7.

Table 1.7 Mechanical properties of the Perspex material used for the model.

Properties	Units	Value
Design modulus (Up to 25°)	Gpa	17
Design stress (Up to 25°)	Mpa	2.5
Density	Kg/m^3	1.19
Coefficient of thermal expansion	K^{-1}	
Poisson's ratio		0.38

Universal joints are used to connect the legs of the tower to the base, while the other end of the leg is connected to the deck. All four legs are fabricated from eight tubes 60 cm long, coupled by an internal ring with a 9 cm diameter and joined with chloroform to make the connection waterproof. Both the top and bottom ends of the tubular legs are covered with two Perspex plates each and made watertight. Subsequently, the four legs are connected to a steel plate at the bottom. One of the legs is furnished with five strain gauges of type FLA-3-350-11 from Tokyo Sokkei Kenkyujo (Japan) at a spacing of every 20 cm, in order to evaluate the strain along the leg. After fixing the strain gauges, waterproofing paste is applied over the strain gauges. Figure 1.31 shows the view of the model with details. Figure 1.32 shows the model of the TMD.

The TMD is chosen to fit the close-resonance band, whose period is given by the following relationship:

$$T = 2\pi\sqrt{\frac{l}{g}} \tag{1.14}$$

Legs of three different lengths are chosen: 12, 19, and 27 cm, which correspond to the periods 0.74, 0.88, and 1.05, respectively. The periods of the TMD with chosen lengths are experimentally evaluated using a potentiometer and an oscilloscope to ensure the design values.

1.11.1 MLAT Without a TMD

Experimental investigations are first carried out on the scale TLP model under wave loads without a TMD. Figure 1.33 shows the free-vibration time history of the tower, with which the natural period of the tower is estimated to be 2.69 seconds; this is also confirmed by the numerical model using the software. Subsequently, the MLAT model is subjected to 3 cycles of waves, each made of 12

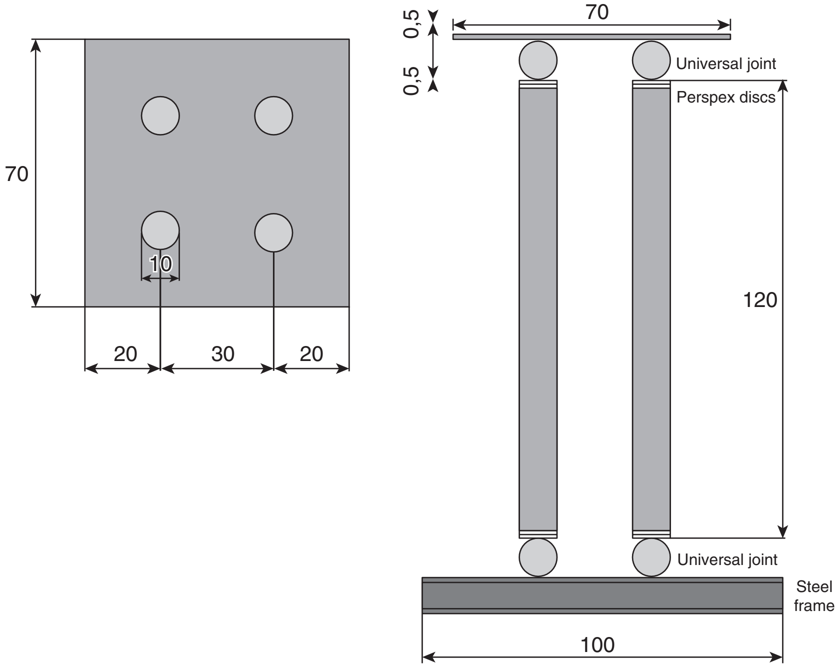

Figure 1.31 Geometric details of the model.

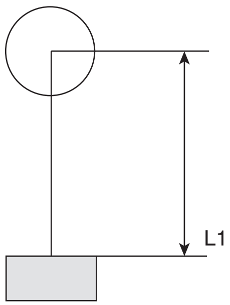

Figure 1.32 Model of a TMD.

waves of different periods: 0.7, 0.8, 0.9, 1.0, 1.1, 2.0, 2.2, 2.4, 2.6, 2.7, 2.8, and 2.9 seconds. Figure 1.34 shows the surge RAO of the tower without a TMD when subjected to three different wave heights. It is seen that surge displacement increases almost linearly up to the first peak, at 2.6 seconds. A kink in the response for all wave heights is attributed to slip that occurred in the tower response, which is characterized by large response amplitudes due to the presence of universal joints. The response further increases at 2.8 seconds with the increase in wave

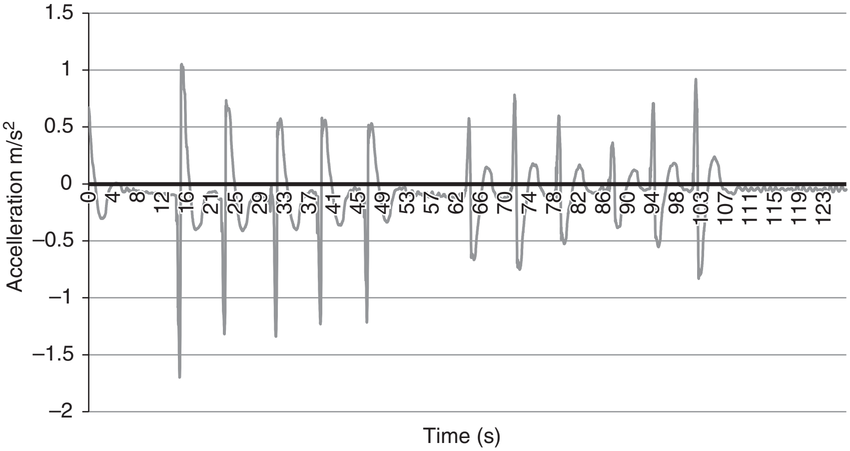

Figure 1.33 Free-vibration time history.

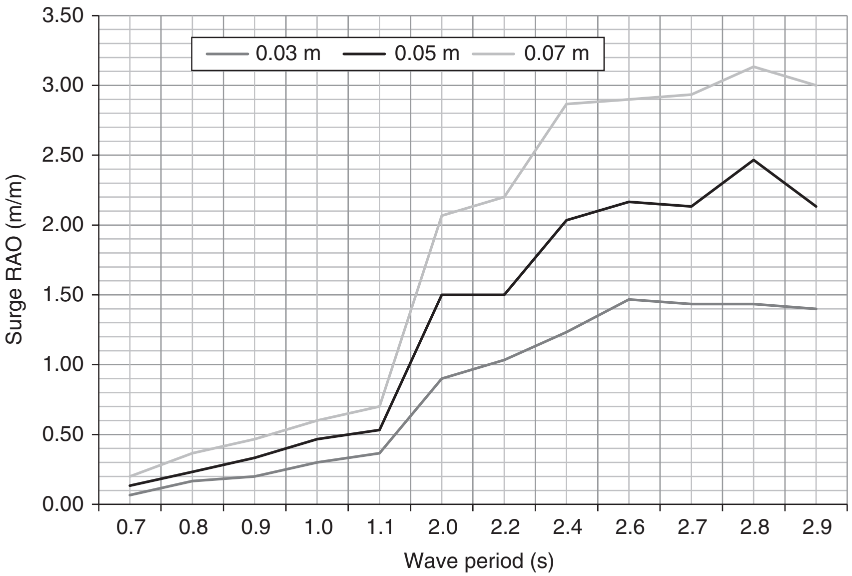

Figure 1.34 Surge response of a MLAT without a TMD.

height. This is explicable because even if the structure is modeled with a single DOF, in the real application, the platform exhibits a MDOF characteristic, showing more than one vibration mode. Hence, the second peak corresponds to the frequency of the structure's second vibration mode.

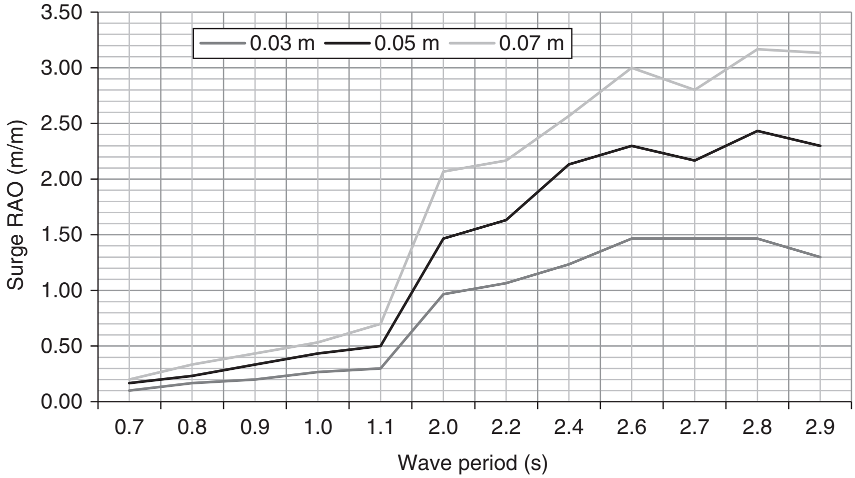

Figure 1.35 Surge RAO for TMD-1.

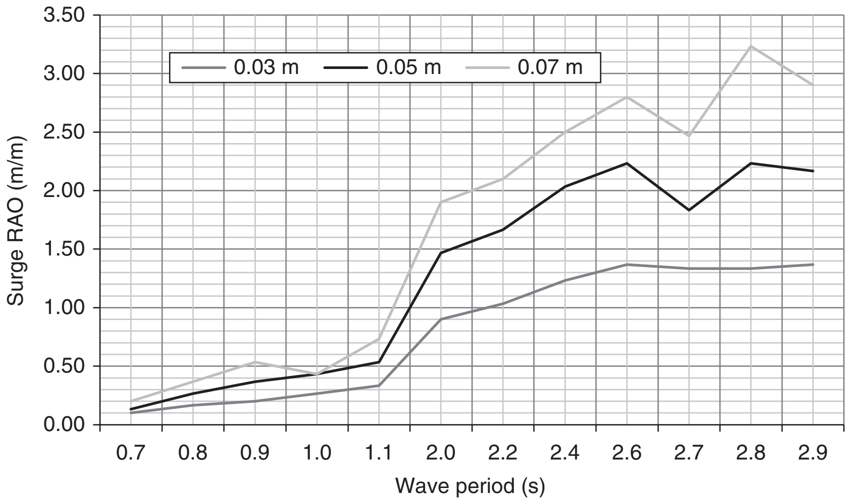

Figure 1.36 Surge RAO for TMD-2.

1.11.2 MLAT with a TMD

The scale model of the MLAT is now investigated in response to regular wave impacts in the presence of a TMD with three chosen configurations, as discussed previously. Figures 1.35–1.37 show surge RAOs for the three TMD configurations, respectively. It is seen that the MLAT fitted with TMD-1 exhibits a response

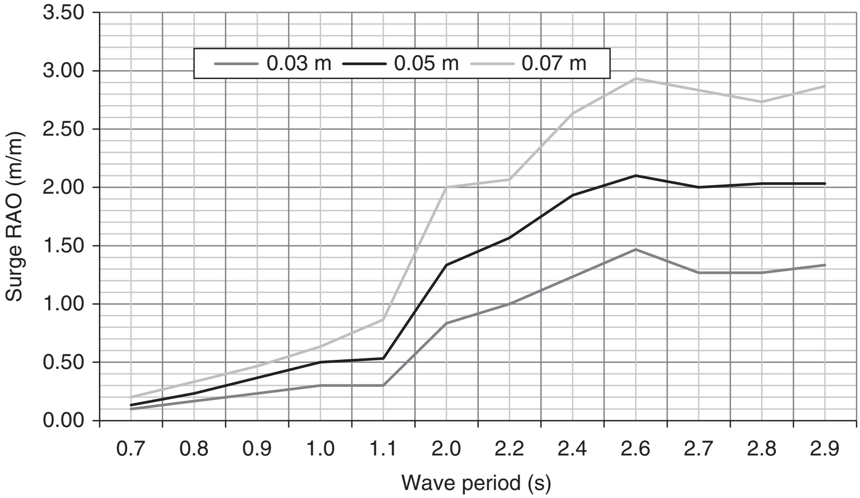

Figure 1.37 Surge RAO for TMD-3.

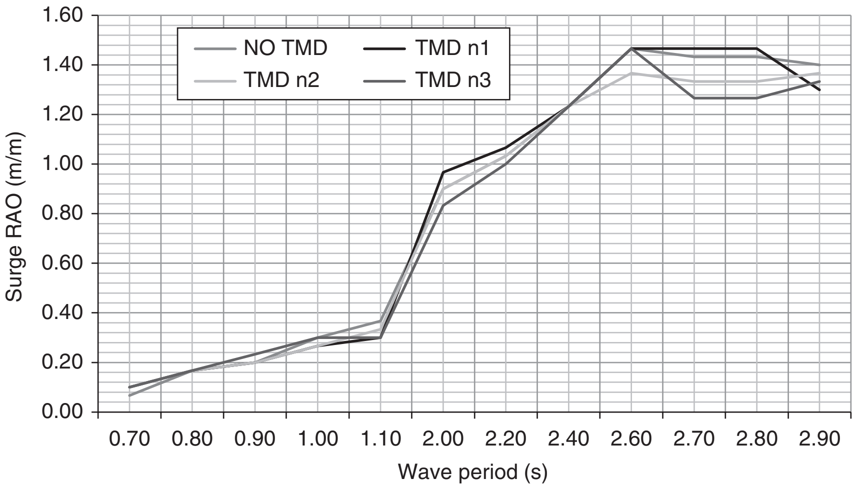

Figure 1.38 Comparison of RAOs for 3 cm wave height.

similar to that in the absence of a TMD; but for other TMD models, response reduction is evident.

In the case of the tower fitted with the TMD-3 model, response reduction is at a maximum, beyond which a TMD will not be effective. Figures 1.38–1.40 compare the response of the MLAT given regular waves 3, 5, and 7 cm high, respectively, for

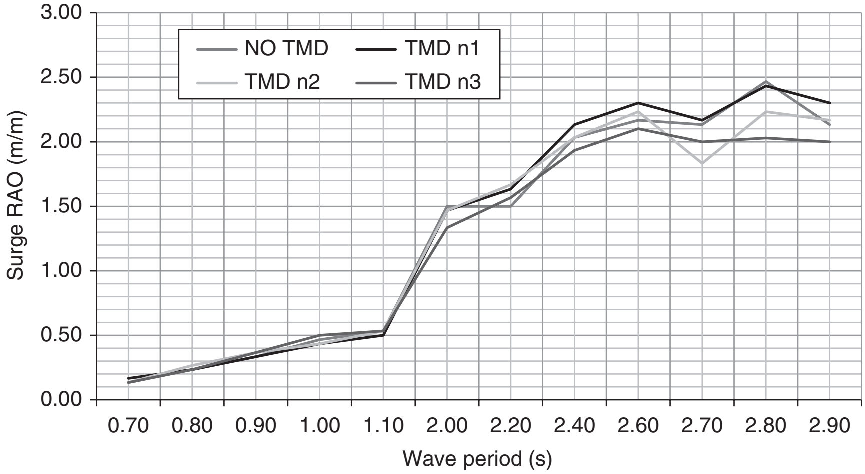

Figure 1.39 Comparison of RAOs for 5 cm wave height.

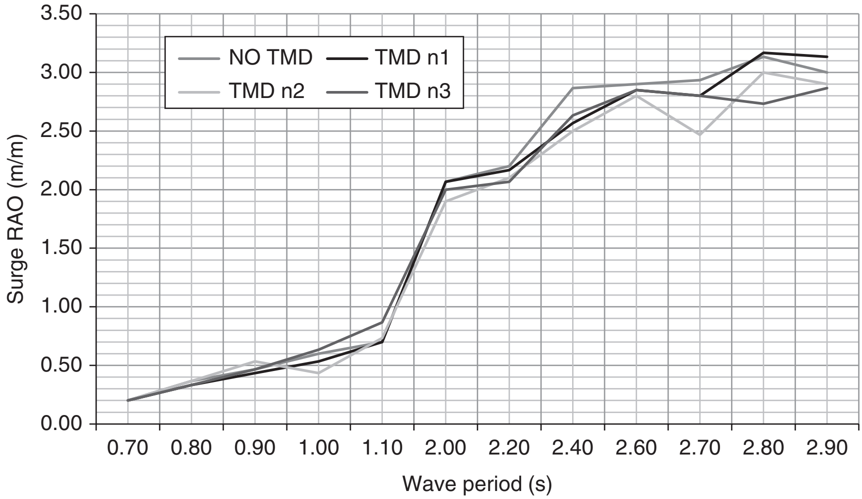

Figure 1.40 Comparison of RAOs for 7 cm wave height.

various periods. It is seen that a TMD attached to the primary system shows an explicit reduction at the period closer to the wave frequency. This shows the effectiveness of tuning the frequency of the damper closer to the resonant frequency band. However, in a case of inappropriate tuning, the response can shoot up, as seen in the case of the tower fitted with TMD-1. However, with the increase in wave height, the response of the tower increases but still depicts the effectiveness of control in the presence of a TMD.